


 Cite this: *RSC Adv.*, 2026, 16, 3478

# Emerging trends and structure–activity insights of Schiff base–lanthanide complexes as antibacterial agents

 Sikandar Paswan, <sup>a</sup> Nitesh Jaiswal, <sup>b</sup> Urvashi, <sup>c</sup> Amar Nath, <sup>a</sup> Manoj Kumar, <sup>d</sup> Divya Mishra <sup>e</sup> and Navneet Yadav <sup>\*c</sup>

The rapid escalation of microbial resistance has accelerated the search for next-generation antibacterial agents with novel mechanisms of action. Schiff bases and their lanthanide complexes have emerged as promising candidates due to their tunable structures, coordination versatility and enhanced bioactivity upon metal binding. While earlier reviews laid the foundational understanding of antibacterial activity of Schiff bases and their metal complexes, this review advances the field by offering a data-driven, mechanistically informed and structure–activity-focused perspective on the most recent antibacterial findings (2018–2025) of Schiff bases and their Ln(III) complexes. In this review article, we critically compare the antibacterial performance of diverse ligand frameworks with lanthanide ions, under varied experimental conditions against both Gram-negative and Gram-positive bacterial strains highlighting trends in structure–activity correlations. We also identify clear trends: Schiff base ligands alone usually show modest or weak antibacterial activity, which is significantly enhanced upon complexation with lanthanide ions. Additionally, unresolved challenges, including toxicity, bioavailability and resistance modulation are discussed alongside proposed future research pathways. This perspective aims to guide the rational design of Schiff base–lanthanide complexes toward clinical translation as potent antibacterial agents.

 Received 25th October 2025  
 Accepted 22nd December 2025

DOI: 10.1039/d5ra08181e

[rsc.li/rsc-advances](https://rsc.li/rsc-advances)

## 1. Introduction

Antimicrobial resistance (AMR) arises when microorganisms including bacteria, fungi, parasites, and viruses adapt and become resistant to the antimicrobial agents used to treat them. Today, AMR is a major global health threat and is projected to cause up to 10 million deaths annually by 2050. Its rapid rise is largely driven by the misuse and overuse of antibiotics in human medicine, agriculture, animal care, and the food industry.<sup>1a,b</sup> Known as the “Silent Pandemic,” AMR is already undermining the effectiveness of existing treatments. Multidrug-resistant pathogens such as MRSA (Methicillin-Resistant *Staphylococcus aureus*), VRE (Vancomycin-Resistant

Enterococci), and CRE (carbapenem-resistant Enterobacteriaceae) are causing increased treatment failures, prolonged illnesses, and higher mortality rates. Since the early antibiotic era, it has been recognized that inappropriate or excessive use accelerates resistance, a problem that has now escalated globally. To combat AMR, international organisations and governments have adopted coordinated strategies, including the “One Health Approach” and the WHO’s Global Action Plan and GLASS surveillance system, which aim to strengthen monitoring and promote responsible antimicrobial use worldwide.<sup>1c,d</sup> The advancement in sanitation, vaccine development and the supplementary public health procedures are insufficient to address the widespread morbidity and mortality caused by infectious diseases. The infections by old diseases and the emergence of new ones have been facilitated due to growing environmental changes, increased transport and human movement, and rising in global warming.<sup>1e,2</sup> Over the past three decades, more than 30 new infectious agents have been discovered worldwide; 60% of which are zoonotic, and more than two-thirds of these have their origins in wildlife.<sup>3</sup> A literature review reported 1407 species of human pathogens, including 208 viruses, 538 bacterial species, 317 fungal species, 57 protozoan species, and 287 helminths. Of these, 177 species (13%) were identified as emerging or re-emerging pathogens, including 77 viruses (37%), 54 bacteria (10%), 22 fungi (7%), 14

<sup>a</sup>Department of Chemistry, Baba Raghav Das Post Graduate College, Deoria, DDU Gorakhpur University, Gorakhpur, U. P. 274001, India

<sup>b</sup>Department of Chemistry, Prof. Rajendra Singh (Rajju Bhaiya) Institute of Physical Sciences for Study & Research, Veer Bahadur Singh Purvanchal University Jaunpur, U. P. 222003, India

<sup>c</sup>Department of Chemical Engineering, Swansea University, Bay Campus, Fabian Way, Swansea SA1 8EN, UK. E-mail: navaneetyadav840@gmail.com; Navneet.yadav@swansea.ac.uk

<sup>d</sup>Department of Chemistry, Government Degree College, Dhadha Bujurg-Hata, Kushinagar, DDU Gorakhpur University, Gorakhpur, U. P. 274207, India

<sup>e</sup>Tumor Microenvironment Unit, Humanitas University, Via Reti Levi Montalcini, 4, 20090 Pieve Emanuele, Milan, Italy


protozoa (25%), and 10 helminths (3%). Emerging and re-emerging infectious diseases account for 26% of annual deaths worldwide.<sup>4-8</sup> Antimicrobial susceptibility screening is widely studied in the drug discovery, epidemiology and prediction of therapeutic outcomes.<sup>9,10</sup> Over the last few decades, scientists achieved great success by reporting several different types of antimicrobial drugs to counter the global public health emergency arising from various G(+) and G(-) bacterial strains.<sup>11-13</sup> The above resistance crisis has not only

undermined the efficacy of frontline therapeutic agents but also emphasized the more research for alternate antimicrobial strategies with novel mechanism of action. The metallo-organic compounds have emerged as main candidates in this search, proposing unique physicochemical properties that often transform into enhanced biological activities.<sup>14</sup> An important organic ligand called Schiff bases, generated by the condensation reaction of primary amines with aldehydes or ketones have attracted significant attention because of their structural



**Sikandar Paswan**

*Dr Sikandar Paswan is an Assistant Professor in the Department of Chemistry at Baba Raghav Das Post Graduate College, Deoria, Uttar Pradesh, India. He qualified for the National Eligibility Test (NET) exam with Junior Research Fellowship (JRF) in Chemical Science, awarded by CSIR-UGC, New Delhi. He earned his DPhil. and MSc degrees in Chemistry from the University of Allahabad and completed his*

*BSc degree in Chemistry from Deen Dayal Upadhyay Gorakhpur University, Gorakhpur. His research interests encompass synthetic inorganic and coordination chemistry, computational chemistry, and their photo-physical and biological applications. Dr Paswan has published several peer-reviewed research articles and book chapters in reputed journals and edited volumes. With over eight years of research and teaching experience, he is actively engaged in higher education and research observation.*



**Nitesh Jaiswal**

*Dr Nitesh Jaiswal is an Assistant Professor (Senior Scale) in the Department of Chemistry at Veer Bahadur Singh Purvanchal University, Jaunpur, India. He earned his PhD and MSc in Chemistry from the University of Allahabad and BSc (Hons.) in Chemistry from Banaras Hindu University. His research interests focuses on synthetic inorganic and coordination chemistry, computational chemistry, and their catalytic and*

*biological applications. He has received research funding from the different government agencies. His academic contributions include peer-reviewed journal articles, edited book, book chapters, and supervision of doctoral and postgraduate research. He is a recipient of the Young Scientist Award from the International Academy of Physical Sciences. He is life member of Indian Science Congress Association, India.*



**Urvashi**

*Miss Urvashi is a PhD researcher in Department of Chemical Engineering, Faculty of Science and Engineering at Swansea University, UK. She is working under the supervision of M. Anji Reddy, whose expertise lies in Materials Engineering. She completed her MSc (Physics) and BSc from the University of Allahabad, India. Her research interests focus on first-principles density functional theory (DFT) based simulations, electronic*

*structure calculations, and computational modelling of materials, particularly for energy materials, ion conducting solids, and electrochemical applications.*



**Amar Nath**

*Dr Amar Nath is an Associate Professor in the Department of Chemistry at Baba Raghav Das Postgraduate College, Deoria, Uttar Pradesh, India. He qualified the National Eligibility Test (NET) examination in Chemical Sciences conducted by CSIR-UGC, New Delhi. He obtained his PhD in Chemistry and Environmental Science from Madan Mohan Malaviya University of Technology, Gorakhpur, and earned his MSc in Chemistry as*

*well as BSc degrees in Chemistry and Botany from Deen Dayal Upadhyay Gorakhpur University, Gorakhpur. His research interests focus on synthetic inorganic chemistry, coordination chemistry, environmental chemistry, and polymer chemistry, with particular emphasis on their environmental applications. Dr Nath has contributed several peer-reviewed research articles and book chapters to reputed journals and edited volumes. He is a Life Member of the Indian Science Congress Association (ISCA), India.*



diversity, ease of synthesis and flexible donor atom sets. Lanthanide–Schiff base complexes exhibit enhanced stability relative to the uncoordinated ligand, due to chelation and electron donation from N O donors.<sup>15</sup> In particular, the incorporation of lanthanide (Ln(III)) ions into Schiff base frameworks



**Manoj Kumar**

*Dr Manoj Kumar completed his BSc in Chemistry from Deen Dayal Upadhyay Gorakhpur University, Gorakhpur, and his MSc (Inorganic Chemistry) from the University of Allahabad, Prayagraj. He was awarded his DPhil. in Chemistry in 2019 from the Department of Chemistry, University of Allahabad, Prayagraj. He is currently serving as an Assistant Professor in the Department of Chemistry, Government Degree College,*

*Dhadha Bujurg (Hata), Kushinagar, India. Dr Kumar has over ten years of research experience in interdisciplinary areas of chemistry. His current research is centered on the design and synthesis of novel transition metal complexes and metal–organic frameworks (MOFs) with applications in catalysis and energy storage devices.*



**Divya Mishra**

*Dr Divya Mishra earned her Master's and PhD degrees in Bioinformatics from the University of Allahabad, Prayagraj, India. Following her doctoral studies, she pursued postdoctoral research at Hadassah Academic College, Jerusalem, Israel, where she worked on the genetic basis of complex diseases with a strong emphasis on computational and integrative omics analyses. She subsequently completed her second postdoctoral fellowship at*

*Humanitas University and Humanitas Research Hospital, Milan, Italy, where her research focused on advanced single-cell and spatial transcriptomics to investigate tumor heterogeneity and immune modulation within the tumor microenvironment. Dr Mishra's research interests encompass single-cell and spatial multi-omics, cancer bioinformatics, immunogenomics, systems biology, and the application of machine learning approaches to biomedical data. She has extensive experience in the analysis of scRNA-seq, spatial transcriptomics, bulk RNA-seq, whole-genome and whole-exome sequencing, and microbiome datasets. She has contributed to multiple peer-reviewed research articles and collaborative interdisciplinary studies. With strong expertise in computational biology and translational cancer research, Dr Mishra continues to actively engage in bioinformatics-driven investigations aimed at understanding disease mechanisms and therapeutic responses.*

has yielded a variety of coordination architectures with notable antibacterial activity.<sup>16</sup> The azomethine (–CH=N–) or an imine (>C=N–) groups present in Schiff bases elucidate the mechanism of transamination and racemisation reaction in biological systems, which makes Schiff bases an important fragment for medical purpose.<sup>17–21</sup> The large ionic radii and unique shielding of 4f orbitals of lanthanide ions offer range of coordination number for metal which allowed the generation of stable mono and poly-nuclear metal complexes. These properties induce superior lipophilicity, and enhanced interaction with bacterial biomolecules compared to the free ligands.<sup>22</sup> Compounds containing lanthanide(III) ions (Ln<sup>3+</sup>) have been of interest since the 19th century. In the 1960s, complexes of the Ln(III) ion exhibiting pharmacological properties such as anticoagulation, anti-inflammatory, antibacterial, anti-allergic and anticancer effects were discovered.<sup>23–26</sup> The antibacterial properties of lanthanide metals were first recognized when Ce(III) salts exhibited antibacterial activity and the oxidizing properties of Ce(IV) led to the use of Ce(IV) sulphate as an antiseptic powder.<sup>27</sup> Consequently, the coordination chemistry of lanthanides and their complexes has attracted significant interest among researchers. The biological properties of Ln(III) ions arise from their similarity to calcium ions, which sparked studies into their potential medical application because Ln<sup>3+</sup> can substitute for Ca<sup>2+</sup> proteins and can influence calcium-dependent enzymes either by inhibiting their function or by enhancing their activation.<sup>28</sup> Additionally, Ln(III) ions such as Nd(III), Sm(III) and Yb(III) ions,



**Navneet Yadav**

*Dr Navneet Yadav earned his Master's and PhD degree in Physics from the University of Allahabad, India. During his doctoral research, he focused on the synthesis and characterization of noble multimetallic nanomaterials for biomedical applications under the supervision of Prof. Raja Ram Yadav. Following his PhD, he was awarded the prestigious Newton International Fellow funded by The Royal Society, London, UK.*

*He successfully completed his postdoctoral research in the Department of Chemical Engineering, Faculty of Science and Engineering at Swansea University. During this fellowship, he broadened his expertise in advanced oxidation processes for environmental remediation and utilized the nanomaterials for the degradation of emerging organic pollutants through the electrochemical oxidation process. His research interests include the synthesis and characterization of nanomaterials for catalytic applications, as well as a wide range of biomedical uses including antibacterial, anticancer, antifungal activities etc. His academic contributions include peer-reviewed journal articles, a patent, book chapters, and supervision of postgraduate students. He is member of Royal Society of Chemistry (MRS\_C\_765719) and Life member of Material Research Society of India (LMB-3663), India.*



are ideal factors for luminescence imaging *in vivo* due to their emission in the NIR region, which can be detected through animal tissue of great thickness.<sup>29–32</sup> Although the potential of Schiff bases and their lanthanide complexes in antibacterial research is well established, the literature still reveals a gap in systematic investigation. An examination of earlier reports reveals a notable gap, suggesting that more comprehensive investigations into structure–activity relationships are required.<sup>33</sup> In particular, limited attention has been devoted to how donor atom sets, substituent effects and coordination numbers influence antibacterial potency. Consequently, the field still lacks a systematic synthesis that links the chemistry of Schiff base–lanthanide complexes with their biological significance.<sup>34–37</sup>

In the present review, we aim to address this gap by providing a comprehensive and focused account of the antibacterial properties of Schiff bases and their lanthanide complexes reported between 2018 and 2025. In contrast to earlier surveys, this work provides new advances in synthesis, coordination features of metal ions, mechanistic insights and antibacterial evaluation into a unified framework that delivers the connection between coordination chemistry and biological outcome. Special attention is given to the comparison of Schiff bases with their corresponding lanthanide complexes, revealing general trends in activity. In addition, the authors have also expressed structure–activity relationships across a wide range of ligands and its Ln(III) complexes which identifies specific structural motifs and coordination environments associated with strong antibacterial activity. Through this approach, the review not only summarizes progress in the field but also clarifies design principles that can inform the rational development of next-generation antibacterial agents. By combining recent literature with comparative and mechanistic analysis, it aims to bridge the disciplines of coordination chemistry and microbiology, thereby offering insights that are both timely and urgently needed in the broader context of combating antibiotic resistance.

## 2. Schiff bases and lanthanide complexes: overview

Schiff bases, first described by Hugo Schiff in 1864, are formed by the condensation of primary amines with aldehydes or ketones and are characterized by the presence of the azomethine ( $-\text{C}=\text{N}-$ ) functional group.<sup>38</sup> Their structural versatility arises from the wide variety of amine and carbonyl precursors, which allows fine-tuning of steric and electronic environments. While the imine nitrogen atom serves as the principal coordination site, additional substituents such as  $-\text{OH}$ ,  $-\text{COOH}$ ,  $-\text{SH}$  and  $-\text{OCH}_3$  increase the denticity of the ligands and enhance the stability of metal complexes.<sup>39</sup> Lanthanide ions, typically in the +II, +III, and +IV oxidation states, are highly electropositive and classified as hard Lewis acids. According to the hard and soft acids and bases (HSAB) principle, they preferentially coordinate with donor atoms such as O, N and S, making Schiff bases ideal ligands for their stabilization. Unlike transition

metals, lanthanides possess shielded 4f orbitals, resulting in weak crystal field effects and predominantly ionic bonding. Nevertheless, Schiff bases stabilize lanthanide center effectively, affording robust and thermally stable complexes that can be mononuclear, binuclear or polynuclear in nature.

Lanthanide coordination chemistry is largely dictated by the large ionic radii of Ln<sup>3+</sup> ions and the steric demands of the coordinating ligands. Because the 4f electrons are effectively shielded and do not participate significantly in bonding, lanthanide–ligand interactions are primarily ionic, leading to high and flexible coordination numbers. With respect to complex formation, lanthanide ions are classified as “Class A” or hard Lewis acids and therefore preferentially bind to hard donor ligands, following the general order  $\text{O} > \text{N} > \text{S}$  and  $\text{F} > \text{Cl}$ . In aqueous solution, Ln<sup>3+</sup> ions are strongly hydrated and form well-defined hydration shells. The number of coordinated water molecules depends on ionic size: the lighter lanthanides typically exhibit higher coordination numbers, commonly forming [Ln(H<sub>2</sub>O)<sub>9</sub>]<sup>3+</sup> species (Ln = La–Eu), while the heavier lanthanides favor lower hydration numbers, most often [Ln(H<sub>2</sub>O)<sub>8</sub>]<sup>3+</sup> (Ln = Dy–Lu). Eu<sup>3+</sup> and Gd<sup>3+</sup> frequently exist as mixed populations with both 8 and 9 coordinate hydration states. This reduction in hydration number across the series is attributed to increasing Ln–O bond strength and decreasing ionic radius, which limit the number of water molecules that can be accommodated. Because of this strong hydration, only ligands capable of forming highly stable chelates can effectively compete with water for coordination in aqueous media.<sup>40a</sup> Bulky ligands such as bis(trimethylsilyl)amine may enforce lower coordination, whereas small, multidentate ligands such as nitrates or macrocycles can stabilize coordination numbers up to 12. A gradual decrease in average coordination number is observed from La to Lu due to the lanthanide contraction, which also shortens Ln–donor distances and influences complex stability, preferred geometries, and ligand selectivity. Oxygen donors dominate the first coordination sphere, followed by carbon donors (mainly from cyclopentadienyl ligands) and nitrogen donors, together comprising roughly 95% of all donor atoms. High-hapticity ligands such as Cp significantly impact both coordination numbers and their variability. Unlike transition metals, lanthanides exhibit minimal ligand field splitting, resulting in limited stereochemical control and a tendency to form irregular coordination geometries such as bicapped trigonal prisms, square antiprisms, and dodecahedra.<sup>40b–d</sup> Their weak ligand field also renders f–f transitions Laporte-forbidden, producing the sharp emission bands characteristic of lanthanide-based luminescent materials. Consistent with HSAB principles, lanthanide ions show strong affinity toward hard donor atoms; thus, oxygen-containing ligands—including carboxylates,  $\beta$ -diketonates, phosphates, and polyoxometalates—form particularly stable complexes. Nitrogen donors such as amines and Schiff bases also coordinate effectively, though generally with slightly reduced stability. These preferences are critical for designing lanthanide-based MOFs, luminescent probes, and antibacterial coordination compounds. Increasing attention is now focused on tuning ligand denticity, steric constraints, and solvent interactions to

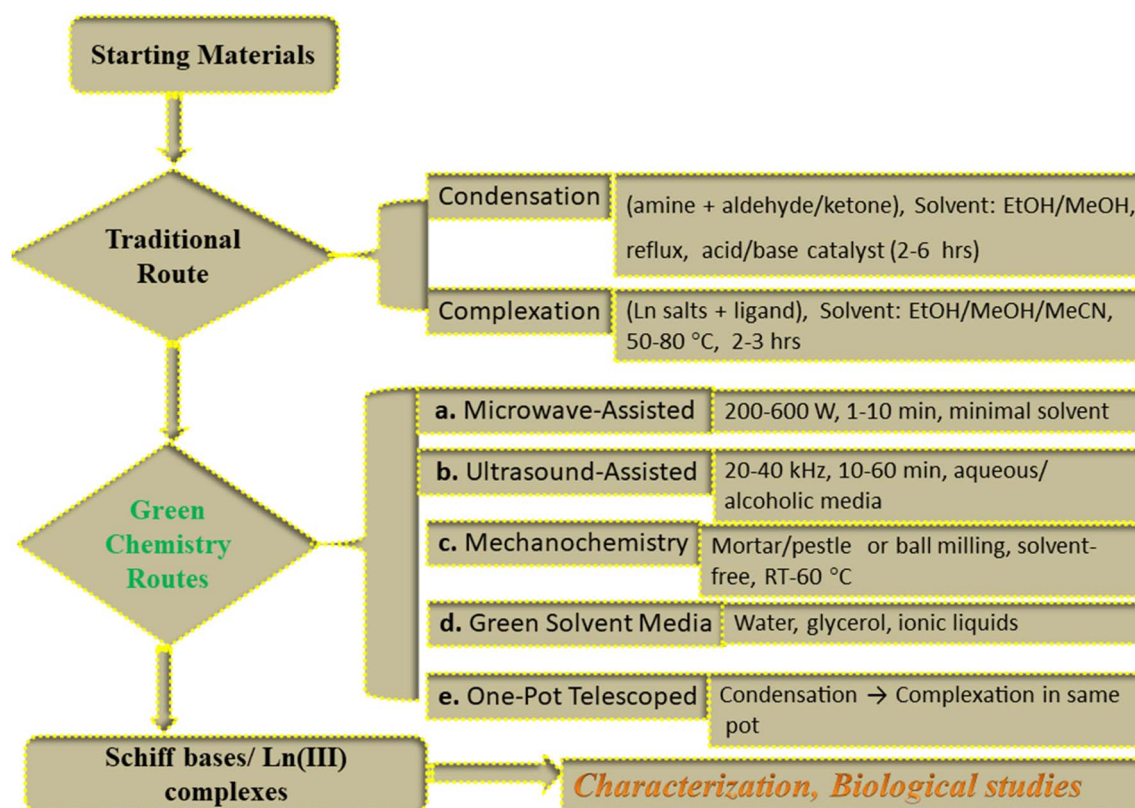


modulate magnetic anisotropy, energy-transfer efficiency, and biological activity. Such structural tunability underpins the versatile applications of lanthanide complexes in catalysis, photophysics, and medicinal chemistry, especially in the development of next-generation antibacterial agents.

Synthesis of Schiff base and its lanthanide complexes typically involve a two-step process: initial condensation of aldehydes and amines, usually in alcoholic solvents such as ethanol or methanol, followed by coordination with hydrated lanthanide salts (nitrates or chlorides). Conventional methods generally employ reflux conditions, which are effective but can be time-consuming and occasionally result in reduced selectivity.<sup>41</sup> In recent years, green chemistry strategies such as solvent-free mechanochemical grinding, microwave-assisted synthesis and ionic liquid-mediated reactions have been explored to reduce reaction times, minimize chemical waste and improve yields. Ethanol remains the most widely used solvent due to its benign and eco-friendly nature; however, greener alternatives are increasingly being adopted in Schiff base and their lanthanide chemistry. In general, the synthetic strategies commonly employed for the preparation of Schiff bases and their lanthanide complexes as reported in various scientific studies are summarized in the following flow chart in Scheme 1.<sup>42–47</sup>

Structurally, Schiff base ligands are particularly suitable for stabilizing lanthanide ions, which owing to their large ionic radii, usually adopt high coordination numbers ranging from 8

to 10 are most common but values of 7 and 11–12 are also observed. The resulting geometries include bicapped trigonal prisms, dodecahedra, and monocapped square antiprisms, with specific arrangements governed mainly by steric and solvation effects rather than crystal field stabilization energy.<sup>48–51</sup> These geometrical features significantly influence the physicochemical properties of the complexes, such as electronic behaviour, lipophilicity, and biological activity. Importantly, the enhanced membrane permeability and lipophilic balance of Schiff base–lanthanide complexes are consistently associated with superior antibacterial activity against both G(+) and G(–) pathogens. In addition, certain systems exhibit dual luminescent and theranostic properties, extending their potential beyond antimicrobial applications to bio-imaging and multifunctional drug design. The structure–activity relationship (SAR) of lanthanide Schiff base complexes, correlating coordination number, donor atom set and antibacterial response against selected pathogens were given in Table 1.<sup>52–55,66,67,92,107,111,115,122,123</sup> The structure–activity relationship (SAR) analysis highlights that Schiff base ligands with amine-derived donor atoms (NOS) play a crucial role in modulating antibacterial potency of Ln(III) complexes. A clear trend is observed where higher coordination numbers (8–10) often correlate with enhanced activity, likely due to increased stability and lipophilicity. Lanthanide identity strongly influences selectivity with Ce(III), Pr(III), Nd(III), Gd(III) and Dy(III) showing broader antibacterial spectra. Overall, the interplay of



Scheme 1 Several routes for the synthesis of Schiff base and their Ln(III) complexes.



**Table 1** Summary of coordination number range, dominant donor fragments, and antibacterial outcomes of lanthanide Schiff base complexes against different pathogens

Sr. no.	Ln(III) ions	Observed coord. no.	Ligand donor features	Amine derived fragments	Pathogens showing enhanced activity
1	Ce(III)	8–10	NO; NN	Aromatic hydrazones; thiazole based amines	SA, LM, BC, PBA
2	Pr(III)	6–10	NO; NN	Hydrazones, ethoxy, pyridyl/phenyl; thiazole, pyridyl	SE, SA, MRSA, EF, PBA, KP, EC, PA
3	Nd(III)	6–10	NO; NN; NOS; NS	Hydrazones, pyridyls, amino phenol; alkyls, thiazoles; benzothiazoles	SA, SE, EC, BS, KP, EF, MRSA, PBA, PV
4	Sm(III)	6–10	NO; NS	Hydrazones, aminophenol, pyridyl, phenyl; benzothiazole	SA, EC, EF, MRSA, KP, SE
5	Eu(III)	7–9	NO; NOS	Hydrazones, phenyls; amino phenols	SE, EC, KP, PA, SA, EF
6	Gd(III)	7–10	NO; NN; NOS; NS	Hydrazones, amino phenols, phenyls; alkyls; benzothiazoles	SA, EC, KP, PA, EF, PV, BS, MRSA, SE
7	Tb(III)	7–9	NO; NOS	Hydrazones, phenyls; amino phenols	SA, SE, KP, PA, EC, EF, MRSA
8	Dy(III)	7–10	NO; NN; NOS	Hydrazones, amino phenols, phenyls; alkyls; benzothiazoles	EC, SA, SAL, BS, ML, EF, MRSA, KP, SE
9	Er(III)	6–10	NO; NN; NOS	Hydrazones, alanines, alkyls; pyridyls, naphthyls, alkyls; benzothiazoles	EC, SA, BS, PA, EF, MRSA, KP, SE, SF
10	Yb(III)	6	NO; NN	Alanine; pyridyl, naphthyls	SA, PA, EC, BS, NG, SF

coordination number, donor environment and Ln(III) ions nature governs antibacterial efficiency against both G(+) and G(−) pathogens.

### 3. Summary of reported antibacterial activity of Schiff bases and Ln(III) complexes

In recent decades, the pursuit of new antibacterial agents has been an active area of research in medicine and pharmacy. Lanthanide complexes, owing to their distinctive electronic configuration, capacity for high coordination number, flexibility in ligand binding and unique physicochemical characteristics have emerged as promising candidates for therapeutic use.<sup>56</sup> Representative examples of lanthanide ions with different Schiff base ligands and their antibacterial activity are presented in Table 1S.

Sogukomerogullari *et al.* (2025)<sup>57–59</sup> synthesized a tridentate NOS donor Schiff base, (H<sub>2</sub>L<sub>1</sub>) by condensing 2,5-thiophenedicarboxaldehyde with 2-aminophenol in MeOH. This ligand was subsequently used to prepare three Ln(III) complexes of the general formula [Ln(L<sub>1</sub>)Cl(H<sub>2</sub>O)]·nH<sub>2</sub>O (Ln = Eu, Tb, Gd). Spectroscopic analyses confirmed a coordination number of seven, involving two nitrogen, two oxygen and one sulfur donor atoms from the ligand, in addition to one aqua and from one chlorido ligand as shown in Fig. 1a. The antibacterial activities of these complexes were evaluated against G(+) strains (SA-ATCC25923, EF-ATCC29212) and G(−) strains (EC-ATCC25922, KP-ATCC700603, PA-ATCC27853) using disk diffusion and broth micro-dilution assays. The complexes consistently displayed higher antibacterial activity compared to the free H<sub>2</sub>L<sub>1</sub> and in some cases were comparable to the standard drug amoxicillin–clavulanic acid (30 μg). Among them, the Eu(III) complex showed the most potent activity, with a 13 mm inhibition zone, MIC of 97.7 μM and MBC of 195.3 μM against

SA. In contrast, the Tb(III) complex demonstrated lower potency (10 mm inhibition against EC; MIC/MBC of 390.7/781.3 μM). The zone of inhibition plots of these complexes against above selected bacterial strains were given in Fig. 8. The enhanced antimicrobial activity of these complexes has been attributed to their increased lipophilicity, resulting from electron delocalization across the chelate ring. This facilitates penetration of bacterial lipid membranes and interference with essential metallo-enzymes by blocking their active sites.<sup>60,61</sup>

Abdel-Fatah *et al.* (2025)<sup>54</sup> prepared a tridentate Schiff base H<sub>2</sub>L<sub>2</sub> by the reaction of 5-bromosalicylaldehyde and 2-amino-3-hydroxypyridine in EtOH and its three lanthanide complexes having general formula [Ln(L<sub>2</sub>)Cl(H<sub>2</sub>O)<sub>2</sub>]·nH<sub>2</sub>O (Ln = Pr, Nd, Sm) as shown in Fig. 2a. Spectral analysis confirm coordination number six of Ln(III) ions involving two oxygen, one nitrogen atoms from Schiff base L<sub>2</sub>, two oxygen from two aqua and one chlorido ligands. The antibacterial activities of these complexes were examined against EC in DMSO solvent by using disk diffusion and dilution methods and results of this study were expressed in diameters of zone of inhibition and in MICs.<sup>27</sup> The metal complexes displayed higher activity compare to free H<sub>2</sub>L<sub>2</sub> and comparable with standard drug ofloxacin. The antibacterial efficacy of the these complexes followed the order ofloxacin > Nd(III) > Pr(III) > Sm(III) > H<sub>2</sub>L<sub>2</sub>.

Zhang *et al.* (2025)<sup>55</sup> using a template-assisted cyclocondensation procedure, prepared two Schiff base macrocyclic mononuclear Ln(III) complexes with a ‘lasso-type’ architecture, having the general formula [Ln(HL<sub>3</sub>)(NO<sub>3</sub>)<sub>3</sub>] (Ln = Pr, Nd). The coordination number of the metal ions in these complexes is ten, arising from four oxygen and two nitrogen donor atoms of the ligand, along with six oxygen atoms from three bidentate nitrate ligands. The antibacterial activity was evaluated against six bacterial strains, including G(+) bacteria (SA, MRSA, EF) and G(−) bacteria (EC, PA, SE), using DMSO as the solvent, and the MIC values were determined by the dilution



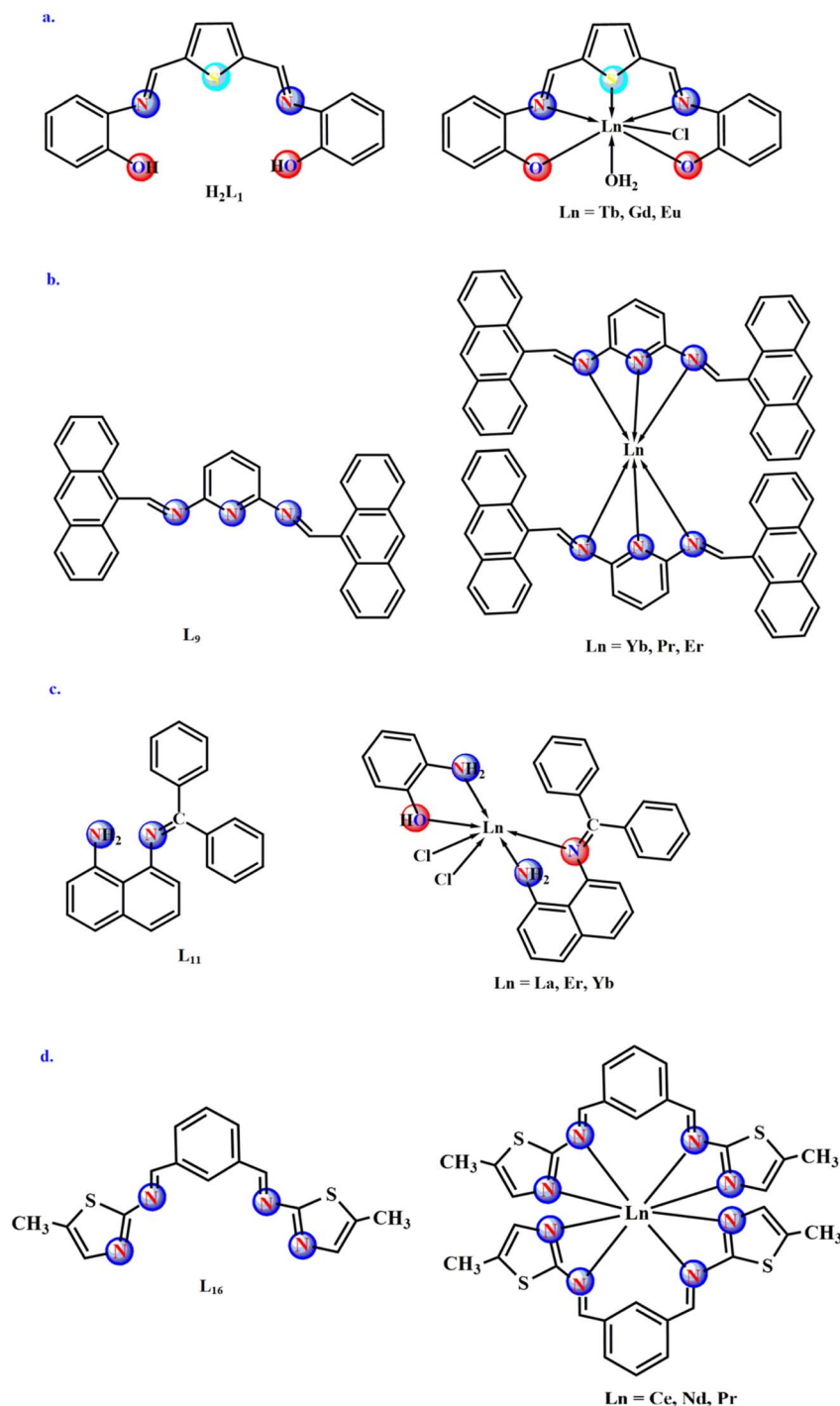


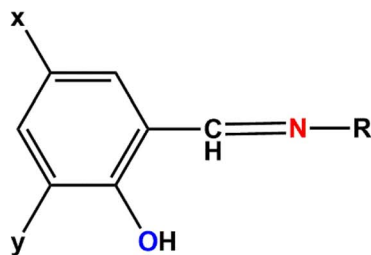
Fig. 1 Structure of Schiff base ligands and their Ln(III) complexes (a–d).

method.<sup>62–64</sup> The results indicated that, due to the synergistic antibacterial effect of the Schiff base and the  $Ln^{3+}$  center, the Pr(III) and Nd(III) complexes exhibited pronounced antibacterial activity against SA, PA, and MRSA, with low MIC values, including  $3.91 \mu g mL^{-1}$  for MRSA.

Abo-Rehab and co-workers (2024)<sup>65</sup> synthesized a Schiff base ( $L_4$ ) through the condensation of 2-aminobenzothiazole with coumarin and this ligand was further used in the preparation of four novel Ln(III) complexes of general formula  $[LnL_4Cl_3] \cdot 2H_2O$

( $Ln = La, Ce, Nd, Dy$ ). Structural analysis indicated that the Ln(III) centers adopt a coordination number of six, involving one nitrogen, one sulfur, and one oxygen donor atom from the Schiff base ligand, along with three chloride ions as shown in Fig. 3a. The antibacterial activities of the free  $L_4$  and its Ln(III) complexes were evaluated using the agar diffusion method against two G(–) (*EC-ATCC10536*, *KP-ATCC10031*) and two G(+) (*SA-ATCC13565*, *BS-DSM1088*). The results, expressed as diameters of zone of inhibition (mm), were compared with the





Sr. No.	x	y	R	Schiff bases (SBs)	Ln(III) complexes	Ref.
a.	Br	H		H <sub>2</sub> L <sub>2</sub>		54
b.	Br	H		H <sub>2</sub> L <sub>5</sub>	-	66
c.				H <sub>2</sub> L <sub>6</sub>		70-71
d.	H	H		HL <sub>8</sub>		74
e.	Cl	H		H <sub>2</sub> L <sub>13</sub>		90
f.	Br	H		H <sub>2</sub> L <sub>14</sub>		
g.	NO <sub>2</sub>	H		H <sub>2</sub> L <sub>20</sub>		107
h.	H	H		H <sub>2</sub> L <sub>21</sub>		110
i.	H	OCH <sub>3</sub>		H <sub>2</sub> L <sub>28</sub>		117

Fig. 2 General structure of salicylaldehyde derived Schiff bases and their Ln(III) complexes (a–i).

standard antibiotic gentamicin. The complexes generally exhibited stronger antibacterial activity than the free ligand, except for the La(III) complex, which displayed comparable

activity. Among the series, the Ce(III) complex showed the highest activity, producing inhibition zones of 21.3 mm (*KP*) and 20.3 mm (*BS*). However, all complexes were less potent than



gentamicin. The observed antibacterial activity followed the order: gentamicin > Ce(III) > Nd(III) > Dy(III) > La(III) > free ligand (L<sub>4</sub>).

Miao *et al.* (2024)<sup>66</sup> published an article dealing with synthesis of H<sub>2</sub>L<sub>5</sub> ligand from 2-(hydroxyimino)propanehydrazide and 5-bromosalicylaldehyde in MeOH and its one

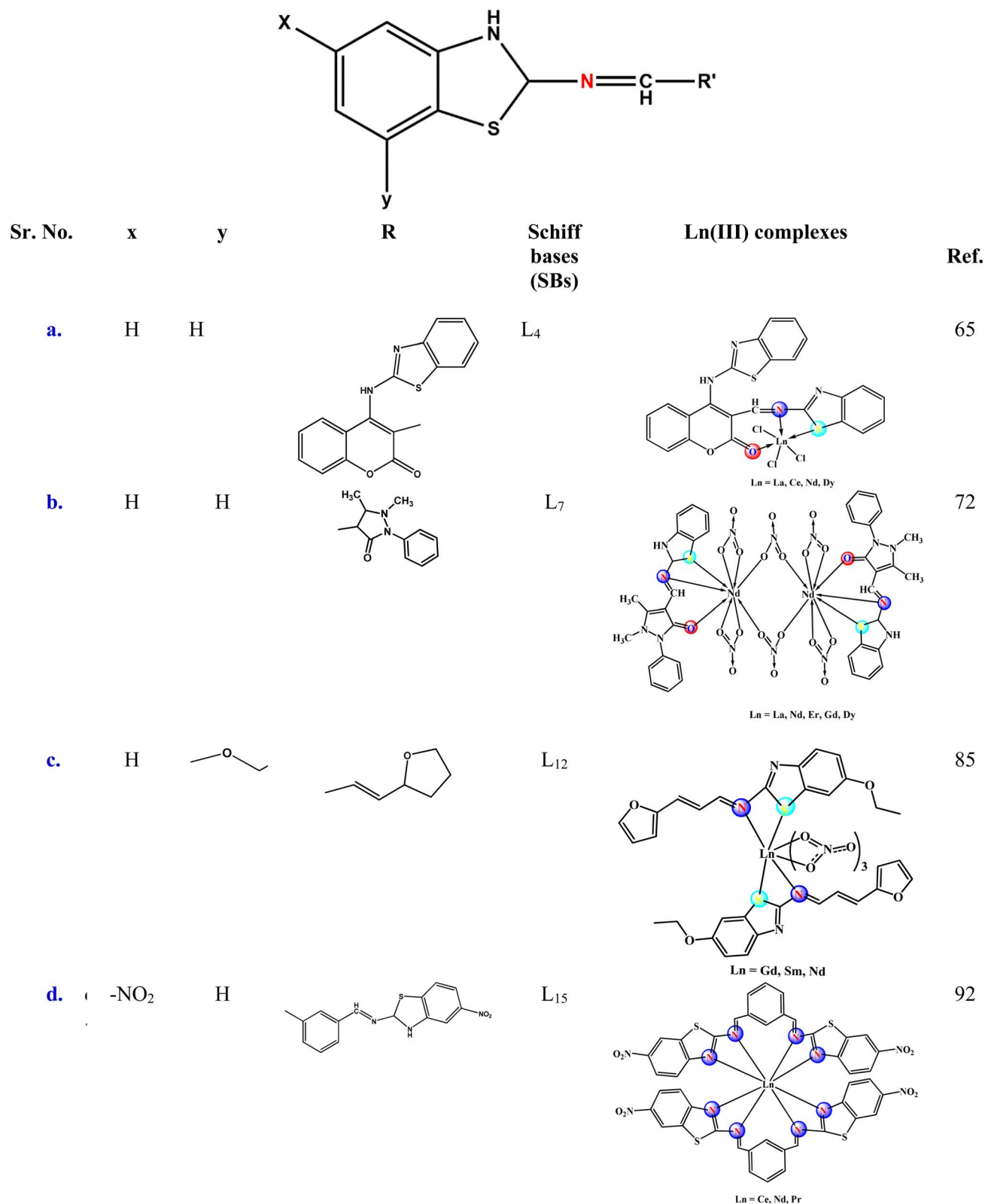


Fig. 3 General structure of aminobenzothiazole derived Schiff bases and their Ln(III) complexes (a–d).



cluster compound  $[\text{Dy}_4(\text{CO}_3)(\text{H}_2\text{L}_5)_4(\text{acac})_2(\text{CH}_3\text{OH})_2(\text{CH}_2\text{OH})_2] \cdot 2\text{CH}_3\text{OH}$ . The structures of ligand are given in Fig. 2b. Single crystal X-ray analysis confirmed coordination numbers eight and nine with geometries triangular dodecahedron and spherical capped square antiprism, respectively. The antibacterial activities of the  $\text{Dy}(\text{acac})_3 \cdot 2\text{H}_2\text{O}$ ,  $\text{H}_2\text{L}_5$  and  $\text{Dy}(\text{III})\text{-H}_2\text{L}_5$  complexes against the five bacteria (*EC*, *SA*, *SAL*, *BS*, *ML*) were evaluated by paper disc diffusion and nutrient broth dilution methods, and results expressed as diameter of zone of inhibition (mm) and MIC, respectively as shown in Fig. 9. The findings demonstrate that  $\text{Dy}(\text{III})$  complex exhibits markedly higher antibacterial activity than both the free ligand  $\text{H}_2\text{L}_5$  and  $\text{Dy}(\text{acac})_3 \cdot 2\text{H}_2\text{O}$  salt. Among the five tested bacteria,  $\text{Dy}(\text{III})$  complex exhibits relatively strong antibacterial activity, with notable inhibition zone diameters of 26.8 mm and 25.5 mm against *SAL* and *ML*, respectively, which is better than 22.7 mm against *EC*, 23.5 mm against *SA*, and 21.5 mm against *BS*. This superior activity is likely due to the Schiff base's complexation with  $\text{Dy}(\text{III})$  ions, which reduces the polarity of the  $\text{Dy}(\text{III})$  ion through partial sharing of its positive charge with the donor groups.<sup>67</sup> The proposed antibacterial mechanism involves disruption of the microbial cell membrane, resulting in intracellular protein denaturation. This process likely inhibits the function of electron-transport enzymes and cell respiration enzymes, ultimately compromising bacterial viability.<sup>68,69</sup>

Taha *et al.* (2024)<sup>70,71</sup> synthesized a Schiff base ligand, ( $\text{H}_2\text{L}_6$ ) via the condensation of 3,5-di-*tert*-butyl-2-hydroxybenzaldehyde with picolinohydrazide in EtOH, and prepared a series of nine lanthanide complexes of the general composition  $[\text{NET}_3]_2[\text{Ln}_2(\text{L}_6)_2(\text{NO}_3)_4] \cdot n\text{H}_2\text{O}$  ( $\text{Ln} = \text{La}, \text{Pr}, \text{Nd}, \text{Sm}, \text{Eu}, \text{Gd}, \text{Tb}, \text{Dy}, \text{Er}$ ). Single-crystal structural studies revealed a coordination number of nine for the  $\text{Ln}(\text{III})$  ions, achieved through three oxygen and two nitrogen donor atoms from the Schiff base and four oxygen atoms from two bidentate nitrate ligands as shown in Fig. 2c and representative ORTEP diagram of  $\text{Dy}(\text{III})$  complex shown in Fig. 11a. The antibacterial activity of the  $\text{H}_2\text{L}_6$  and its  $\text{Ln}(\text{III})$  complexes was investigated against three  $\text{G}^+$  (*SA*, *MRSA*, *EF*) and three  $\text{G}^-$  (*KP*, *EC*, *SE*) using both the micro-broth dilution and disk diffusion methods, with amoxicillin as the reference drug. The free ligand  $\text{H}_2\text{L}_6$  and most complexes showed moderate antibacterial activity, predominantly against  $\text{G}^-$  bacteria. Notably,  $\text{Eu}(\text{III})$ ,  $\text{Nd}(\text{III})$  and  $\text{Pr}(\text{III})$  complexes demonstrated enhanced activity against *SE* with a MIC of  $64 \mu\text{g mL}^{-1}$ , compared to the free ligand (MIC  $128 \mu\text{g mL}^{-1}$ ). However, none of the compounds were effective against  $\text{G}^+$  strains, and all exhibited lower activity than the standard antibiotic. The authors attributed the improved activity of selected  $\text{Ln}(\text{III})$  complexes to Overtone's concept of cell permeability, where chelation increases lipophilicity, facilitating transport across bacterial membranes. The differential response between  $\text{G}^+$  and  $\text{G}^-$  strains was explained by differences in cell wall architecture:  $\text{G}^+$  bacteria possess a thick peptidoglycan wall, while  $\text{G}^-$  bacteria have a thinner peptidoglycan layer combined with an outer lipopolysaccharide membrane, which influences permeability and susceptibility to antimicrobial agents.

Hussein *et al.* (2024)<sup>72</sup> synthesized a Schiff base, ( $\text{L}_7$ ) through the condensation of 4-antipyrinecarboxaldehyde with 2-aminobenzothiazole and a series of lanthanide complexes of general formula  $[\text{Ln}_2(\text{L}_7)_2(\text{NO}_3)_6] \cdot 6\text{H}_2\text{O}$  ( $\text{Ln} = \text{La}, \text{Nd}, \text{Er}, \text{Gd}, \text{Dy}$ ). Spectroscopic analysis confirmed that the  $\text{Ln}(\text{III})$  ions adopt a nine-coordinate geometry, with donor atoms contributed by one nitrogen, one sulfur, and one oxygen from the ligand, along with six oxygen atoms from four nitrate ligands (Fig. 3b). The antibacterial activity of the ligand and its complexes was evaluated against two  $\text{G}^+$  (*SA*, *BS*) and two  $\text{G}^-$  (*EC*, *KP*) strains using the disk diffusion method. Against *SA*,  $\text{Er}(\text{III})$  (30 mm),  $\text{Gd}(\text{III})$  (33 mm) and  $\text{Dy}(\text{III})$  (31 mm) complexes exhibited higher activity than the free ligand (26 mm), while  $\text{Nd}(\text{III})$  (26 mm) was comparable and  $\text{La}(\text{III})$  (20 mm) was less active. For *BS*,  $\text{Er}(\text{III})$  (29 mm),  $\text{Gd}(\text{III})$  (30 mm), and  $\text{Nd}(\text{III})$  (25 mm) showed improved activity relative to the ligand (24 mm), whereas  $\text{Dy}(\text{III})$  (20 mm) and  $\text{La}(\text{III})$  (22 mm) were less effective. Against *EC*, most complexes demonstrated activity similar to the free ligand, except  $\text{Gd}(\text{III})$  and  $\text{Dy}(\text{III})$ , which were more active. Remarkably, both the ligand and all complexes exhibited strong antibacterial effects against *KP*, with the  $\text{Nd}(\text{III})$  complex showing the highest inhibition zone of 34 mm. The authors attributed the enhanced antibacterial activity of  $\text{Ln}(\text{III})$ -Schiff base complexes to their ability to disrupt bacterial cell membranes, leading to increased permeability, leakage of intracellular components, and ultimately cell death.<sup>73</sup>

Alqasaimah *et al.* (2023)<sup>74</sup> synthesized a Schiff base, ( $\text{HL}_8$ ) by condensation reaction of salicylaldehyde with *p*-toluidine and its three  $\text{Ln}(\text{III})$  complexes of the general formula  $[\text{Ln}(\text{HL}_8)_3(\text{NO}_3)_3]$  ( $\text{Ln} = \text{Nd}, \text{Tb}, \text{Dy}$ ) (Fig. 2d). The coordination number of  $\text{Ln}(\text{III})$  ions is nine, six from three bidentate nitrate ions and three from three  $\text{HL}_8$ . The representative ORTEP diagram of  $\text{Nd}(\text{III})$  complex shown in Fig. 11b. The authors investigated antibacterial properties of these complexes against  $\text{G}^+$  (*SA-ATCC29213*, *SA-ATCC33591*) and  $\text{G}^-$  (*EC-ATCC25922*, *PA-ATCC27853*) using the disk diffusion; diameter of zone of inhibition (mm) and micro-dilution methods; MIC with gentamicin and amikacin as reference drugs. The results showed that  $\text{HL}_8$  exhibits no zone of inhibition against all bacteria strains whereas its  $\text{Ln}(\text{III})$  complexes shows some sensitivity against *SA-ATCC29213* and *EC-ATCC25922* except other bacterial strains *SA-ATCC33591* and *PA-ATCC27853*. All the  $\text{Ln}(\text{III})$  complexes with MIC  $0.75 \text{ mg mL}^{-1}$  against *SA-ATCC29213* is very efficient than free Schiff base.

Andiappan *et al.* (2023)<sup>75</sup> reported a Schiff base ( $\text{L}_9$ ) through the condensation reaction of 9-anthraldehyde with 2,6-diaminopyridine in MeOH and their three  $\text{Ln}(\text{III})$  complexes ( $\text{Ln} = \text{Yb}, \text{Pr}, \text{Er}$ ) as shown in Fig. 1b. Antibacterial performance was evaluated against  $\text{G}^+$  (*SA*) and  $\text{G}^-$  (*PA*) using the well diffusion method (zone of inhibition, mm) and microdilution analysis (MIC,  $\mu\text{g mL}^{-1}$ ) at concentrations of 20, 40, 60, and  $80 \mu\text{g mL}^{-1}$ . Against *PA*, the free ligand showed inhibition zones of 10, 12, 12, and 14 mm across the tested concentrations, while the  $\text{Pr}(\text{III})$  complex exhibited markedly enhanced activity with zones of 18, 22, 24, and 24 mm. This activity was comparable to the standard antibiotic streptomycin, which produced a 25 mm inhibition zone. Against *SA*, the free ligand (20 mm)



demonstrated moderate activity, which was further improved in its complexes: Pr(III) (24 mm), Er(III) (21 mm), and Yb(III) (22 mm). The antibacterial activity data of these complexes at various concentrations against both strains were given in Fig. 10. The results highlight that complexation with Ln(III) ions significantly enhances the antibacterial properties of the Schiff base ligand, with the Pr(III) complex emerging as the most potent candidate, approaching the activity of the standard drug. The improved bioactivity was attributed to increased lipophilicity of the complexes, facilitating greater bacterial membrane penetration and interaction with intracellular targets.<sup>76,77</sup>

Xue *et al.* (2023)<sup>78</sup> synthesized a Schiff base ligand, H<sub>2</sub>L<sub>10</sub> via the condensation of 5-hydroxypyridine-2-carbohydrazide with 6-methoxypyridine-2-carbaldehyde in MeOH, and subsequently

prepared three trinuclear Ln(III) complexes of the general formula [Ln<sub>3</sub>(dbm)<sub>5</sub>(L<sub>10</sub>)<sub>2</sub>(CH<sub>3</sub>OH)]CH<sub>2</sub>Cl<sub>2</sub> (Ln = Nd, Sm, Tb) through reaction with dibenzoylmethane (dbm) salts of lanthanides, Ln(dbm)<sub>3</sub>·2H<sub>2</sub>O (Fig. 4a). Single-crystal X-ray diffraction confirmed that the complexes adopt multinuclear architectures, with coordination numbers of 8 and 9 around the Ln(III) centres. The representative ORTEP diagrams of Sm(III) and Tb(III) complexes are shown in Fig. 11c and d. Antibacterial activity was evaluated against G(−) (*PSy*) using both agar diffusion (zone of inhibition) and broth dilution (MIC) methods, with DMF as solvent.<sup>79–82</sup> The results demonstrated that the complexes displayed enhanced antibacterial efficacy (24–27 mm inhibition zone), particularly for Tb(III) (27.5 mm), compared to the free ligand H<sub>2</sub>L<sub>10</sub> (22 mm) and the parent metal salts Ln(dbm)<sub>3</sub>·2H<sub>2</sub>O (16–17.5 mm). These findings

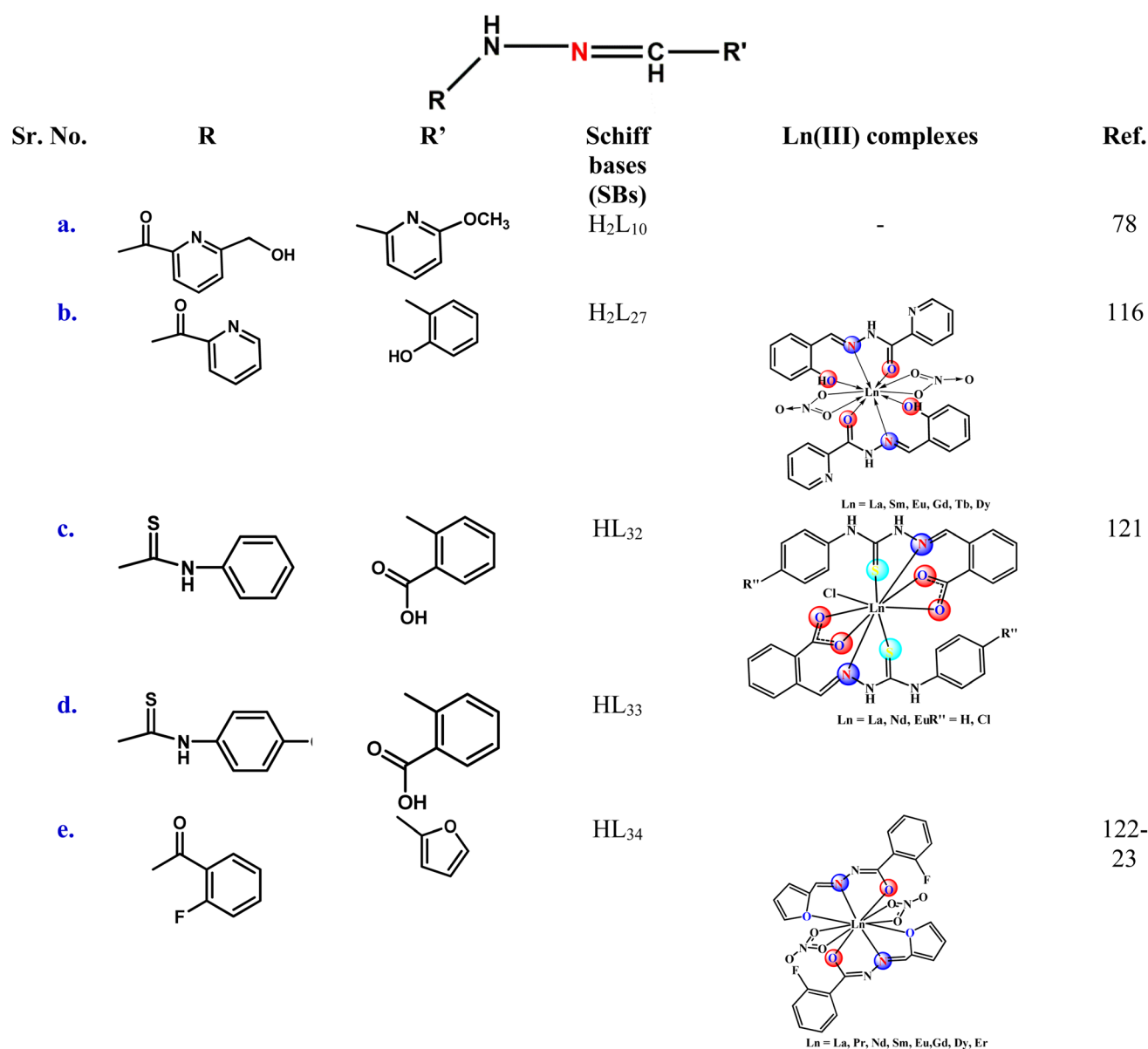


Fig. 4 General structure of hydrazide derived Schiff bases and their Ln(III) complexes (a–e).



indicate that complexation with Ln(III) ions significantly improves the antibacterial potency of Schiff bases, with Tb(III) showing the strongest effect, likely due to favourable coordination geometry and higher redox activity facilitating bacterial membrane disruption.

Khalil and Mohamed (2023),<sup>83</sup> synthesized a Schiff base (L<sub>11</sub>) *via* condensation of benzophenone with naphthalene-1,8-diamine and its mixed-ligand lanthanide complexes through coordination with *o*-aminophenol and Ln(III) salts, affording compounds of the type [Ln(L<sub>11</sub>)(*o*-AP)Cl<sub>2</sub>]Cl *n*H<sub>2</sub>O (Ln = La, Er, Yb). Structural analysis revealed a coordination number of six, with Ln(III) centers bound by two nitrogen donors from L<sub>11</sub>, one oxygen, one nitrogen atom from *o*-AP, and from two chlorido ligands (Fig. 1c). The antibacterial activities were evaluated against G(+) (*BS*) and G(−) (*EC*) strains using the disc diffusion method, with gentamicin and ampicillin as standard ref. 84 The results demonstrated that all Ln(III) complexes displayed higher antibacterial activity than the free Schiff base (L<sub>11</sub>), though slightly weaker than *o*-aminophenol alone. The order of potency was: ampicillin > *o*-AP > La(III) = Er(III) = Yb(III) > L<sub>11</sub> (against *BS*), and *o*-AP > gentamicin > La(III) = Er(III) = Yb(III) > L<sub>11</sub> (against *EC*). These findings indicate that while the Ln–Schiff base complexes exhibit moderate enhancement over the parent ligand, their activity remains below that of standard antibiotics, highlighting scope for further ligand modification to optimize antibacterial performance.

Abu-Yamin and co-workers (2022)<sup>85</sup> prepared a Schiff base, (L<sub>12</sub>) by the condensation reaction of 3-(2-furyl)acrolein with 2-amino-6-ethoxybenzothiazole in EtOH solvent and their three lanthanide complexes of composition [Ln(L<sub>12</sub>)<sub>2</sub>(NO<sub>3</sub>)<sub>3</sub>] (Ln = Gd, Sm, Nd). They were tested their antibacterial activity against both G(+) (*SA*-ATCC25923, *BS*-RCMB015) and G(−) (*EC*-ATCC25922, *PV*-RCMB004) bacterial strain. The lanthanide ions possess ten coordination number by six oxygen atoms from three bidentate nitrate ions and two oxygen, two nitrogen atoms from two L<sub>12</sub> ligands as shown in Fig. 3c. The results antibacterial activity of these complexes was expressed in MIC by using broth micro-dilution method and compared these results with standard drug gentamicin. The results showed that lanthanide complexes expressed higher antibacterial activity than free Schiff base and lower than gentamicin. The results showed that Nd(III) complex possess greater activity than free Schiff base and other two La(III) and Sm(III) complexes and these value comprised with previous antibacterial results. The authors concluded that the enhanced activity of lanthanide complexes than free Schiff base is due to higher lipophilicity of the Ln(III) ions and also by inhibition of growth of microbes by blocking their active mechanisms.<sup>86–89</sup>

Taha *et al.* (2022)<sup>90</sup> were synthesized two Schiff base ligands, H<sub>2</sub>L<sub>13</sub> and H<sub>2</sub>L<sub>14</sub> through condensation of 5-chlorosalicylaldehyde and 5-bromosalicylaldehyde, respectively with 2-fluorobenzoic hydrazide. Each ligand was further used to prepare a series of nine Ln(III) complexes with the general composition [Ln(H<sub>2</sub>L<sub>13–14</sub>)(NO<sub>3</sub>)<sub>2</sub>(H<sub>2</sub>O)] (Ln = La, Pr, Nd, Sm, Eu, Gd, Tb, Dy, Er). Spectroscopic characterization revealed that the Ln(III) ions adopt an eight-coordinate environment, involving two oxygen and one nitrogen donor atoms from the

Schiff base ligand, four oxygen atoms from two bidentate nitrate ligands, and one oxygen from a coordinated aqua as shown in Fig. 2e and f. The antibacterial activities of the free ligands H<sub>2</sub>L<sub>13</sub> and H<sub>2</sub>L<sub>14</sub> and their Ln(III) complexes were evaluated against G(+) (*EF*, *SA*, *MRSA*) and G(−) (*EC*, *KP*, *SE*) bacterial strains using the micro-broth dilution method, with amoxicillin as the reference drug.<sup>91</sup> The results demonstrated that the Ln(III) complexes generally exhibited stronger antibacterial activity than the free Schiff bases and, notably, showed superior inhibitory effects compared to the reference drug against *EF*. Furthermore, the H<sub>2</sub>L<sub>14</sub>-derived lanthanide complexes displayed higher antibacterial potency than their H<sub>2</sub>L<sub>13</sub> analogues, indicating that the introduction of a bromine substituent on the aromatic ring enhances antimicrobial efficacy.

Mishra *et al.* (2020)<sup>92</sup> reported the synthesis of two new tetradentate Schiff base ligands, L<sub>15</sub> and L<sub>16</sub>, derived from the condensation of 5-nitrobenzothiazole and 2-amino-5-methylthiazole, respectively, with 1,3-benzenedicarboxaldehyde in EtOH. These ligands were further employed to prepare six Ln(III) complexes of the general compositions [Ln(L<sub>15</sub>)<sub>2</sub>] and [Ln(L<sub>16</sub>)<sub>2</sub>] (Ln = Ce, Nd, Pr) by reacting the ligands with the respective lanthanide nitrate salts in a 1:2 molar ratio. Spectroscopic analyses confirmed that the Ln(III) ions adopt an eight-coordinate environment involving eight nitrogen atoms from two ligands in both series of complexes as shown in Fig. 3d and 1d. The antibacterial activities of the free ligands and their complexes were evaluated using the agar diffusion method against two G(+) bacteria (*SA*, *PBA*). The results revealed that the Ln(III) complexes exhibited higher antibacterial potency than the corresponding Schiff bases, particularly against *SA* (responsible for skin infections and food poisoning) and *PBA* (a major cause of acne). These findings suggest that coordination with Ln(III) ions enhances the antimicrobial efficiency of the Schiff bases by improving lipophilicity and membrane permeability.<sup>93–95</sup>

Deghadi *et al.* (2022)<sup>96–98</sup> synthesized two Schiff base ligands, L<sub>17</sub> and HL<sub>18</sub> obtained by the reaction of 1,8-naphthalenediamine and alanine, respectively with 2-acetylferrocene as shown in Fig. 5a. These Schiff bases were further used for the preparation of six new lanthanide(III) complexes of general formula [Ln(L<sub>17</sub>)(H<sub>2</sub>O)<sub>2</sub>Cl<sub>2</sub>] and [Ln(HL<sub>18</sub>)(H<sub>2</sub>O)<sub>(1–3)</sub>Cl<sub>(1–3)</sub>] (Ln = La, Er, Yb). All the synthesized Ln(III) complexes adopt octahedral geometry. The authors evaluated the antibacterial activity of these complexes against four G(+) (*SA*, *BC*, *BS*, *SF*) and four G(−) (*EC*, *PA*, *NG*, *ST*) bacterial strains in term of zone of inhibition by using disc diffusion method,<sup>99</sup> with DMF as negative control and gentamicin as a positive standard. The results showed that Yb(III) complexes of L<sub>17</sub> Schiff base exhibited enhanced activity compare to free ligand L<sub>17</sub> against *NG* and *SF* bacterial strains.

Hussein and Shaalan (2022)<sup>100</sup> reported a Schiff base, L<sub>19</sub> by the reaction of 4,4-methylenediantipyrine with ethylenediamine in EtOH and their five new lanthanide complexes of the general formula [Ln(L<sub>19</sub>)<sub>2</sub>(NO<sub>3</sub>)<sub>3</sub>] (Ln = Nd, La, Er, Gd, Dy). Four nitrogen atoms from two Schiff base ligands and six oxygen atoms from three bidentate nitrate ions provide coordination



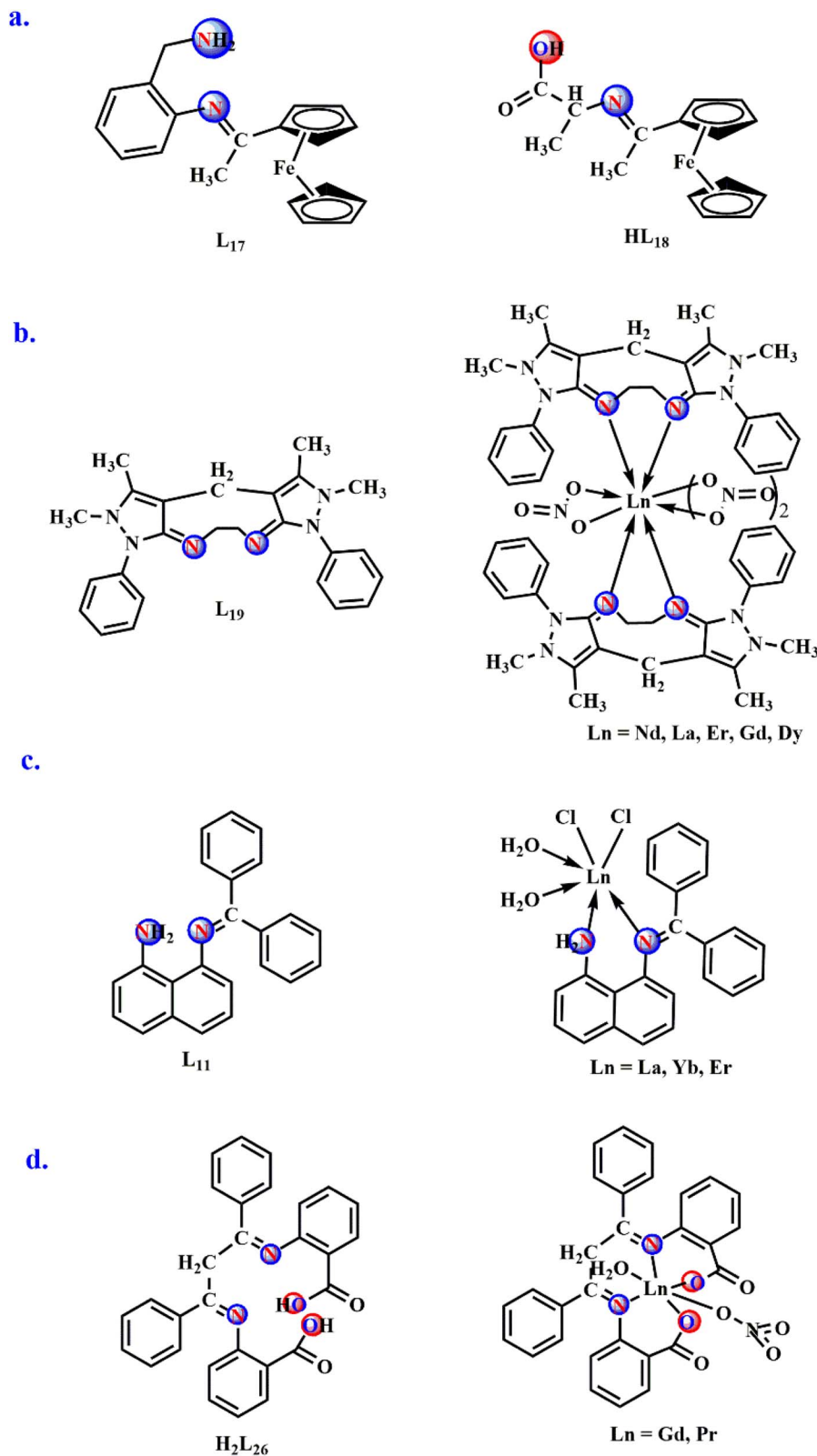


Fig. 5 Structure of Schiff base ligands and their Ln(III) complexes (a–d).

number ten for the lanthanide ions in complexes (Fig. 5b). The authors reported the antibacterial activity of these complexes against two G(–) bacteria (*EC*, *KP*) and two G(+) bacteria (*SA*, *BS*)

by utilizing disc diffusion method. The activity of complexes reveals that the majority of lanthanide complexes exhibited higher activity as compared to free L<sub>19</sub>. This research indicates



that most of lanthanide complexes are more effective against *SA* followed by *BS* than *G(-)* bacteria. The lanthanide complexes showed more powerful activity against *KP* than *EC*. Although all bacteria have an inner cell membrane, *G(-)* bacteria have a distinct outer membrane, which is responsible for the increased resistance to antibacterial treatments in these pathogen's cell. This outer layer keeps a number of medications and antibiotics from penetrating the cell.<sup>101–103</sup>

Khalil and his co-workers (2021)<sup>104</sup> also uses Schiff base, *L*<sub>11</sub> for the synthesis of another three lanthanide complexes of composition  $[\text{Ln}(\text{L}_{11})(\text{H}_2\text{O})_2\text{Cl}_2]\text{Cl}$  (*Ln* = La, Yb, Er). These Ln(III) complexes were adopt octahedral geometry involving two chlorido, two oxygen from two aqua molecules and two nitrogen atoms from *L*<sub>11</sub> as shown in Fig. 5c. The antibacterial activity of ligand and its Ln(III) complexes against *G(+)* (*BS*) and *G(-)* (*EC*) strains were evaluated by using disc diffusion method with gentamycin and ampicillin as standard drugs.<sup>99</sup> The results showed that Ln(III) complexes as compared to free *L*<sub>11</sub> displayed higher activity against both strains according to this order as ampicillin > Er(III) > La(III) > Yb(III) = *L*<sub>11</sub> > for *BS* and gentamicin > Er(III) > La(III) = Yb(III) = *L*<sub>11</sub> for *EC*. Overtone's concept and Chelation theory might be used to explain why metal complexes have increased activity.<sup>105,106</sup>

Another series of lanthanide Schiff base complexes have been published by Taha *et al.* (2021),<sup>107</sup> by using an important organic compound (*H*<sub>2</sub>*L*<sub>20</sub>) which have composition  $[\text{Ln}(\text{L}_{20})(-\text{NO}_3)(\text{H}_2\text{O})] \cdot n\text{H}_2\text{O}$  (*Ln* = La, Pr, Nd, Sm, Eu, Gd, Tb, Dy). The tetradentate ligand (*H*<sub>2</sub>*L*<sub>20</sub>) obtained by the reaction of phenylenediamine and 5-nitrosalicylaldehyde in EtOH. The coordination number of Ln(III) ions in their complexes is seven achieved by two nitrogen, two oxygen atoms from *H*<sub>2</sub>*L*<sub>20</sub>, two oxygen atoms from one bidentate nitrate ions and one oxygen atom from one aqua ligand (Fig. 2g). The antibacterial investigation of these complexes was performed against *G(-)* (*SE*, *KP*, *EC*) and *G(+)* (*SA*, *MRSA*, *EF*) strains using micro-broth dilution method and results expressed in term of MIC<sup>108</sup> with amoxicillin as a reference drug. On the basis of MIC values, the free *H*<sub>2</sub>*L*<sub>20</sub> showed less activity against all tested bacterial strains except *SA* and *MRSA* for which *H*<sub>2</sub>*L*<sub>20</sub> alone showed approximately higher activity than amoxicillin. The most noticeable inhibitory activity was observed in case of La(III) and Pr(III) complexes against *KP*, *SA* and *MRSA*. The Dy(III) complex had higher activity than amoxicillin for *EF* and *MRSA*. Finally the authors concluded that with few exceptions, lanthanide(III) complexes were more active on *G(+)* bacterial strains than on *G(-)* bacterial strains. The enhanced activity against *G(+)* bacteria may be due to their increased susceptibility to antibiotics due to the lack of an outer low-permeability barrier.<sup>109</sup>

Hussein (2021),<sup>110</sup> synthesized a tetradentate Schiff base (*H*<sub>2</sub>*L*<sub>21</sub>) by the reaction of salicylaldehyde and ethylenediamine in EtOH solvent which is further used in the preparation of europium complex of composition  $[\text{Er}(\text{H}_2\text{L}_{21})(\text{NO}_3)_2]\text{NO}_3$ . The reported coordination number of Er(III) ion is eight involving two nitrogen, two oxygen atoms from Schiff base and four oxygen atoms from two bidentate nitrate ions (Fig. 2h). The author evaluated the antibacterial activity of complexes by using *EC* and *SA* bacterial strains in term of zone of inhibition. The

results showed that antibacterial activity of erbium complex is greater than free Schiff base.

Muriel *et al.* (2021)<sup>111</sup> reported four bidentate Schiff base ligands *HL*<sub>22</sub>, *HL*<sub>23</sub>, *HL*<sub>24</sub>, *HL*<sub>25</sub> derived from 2-(*m*-aminophenyl) benzimidazole, 2-(*p*-aminophenyl)benzimidazole, salicylaldehyde, 2,4-dihydroxybenzaldehyde and its eight lanthanide complexes having composition  $[\text{Ln}(\text{L}_{22-25})_2\text{Cl}(\text{H}_2\text{O})_m] \cdot n\text{H}_2\text{O}$  (*Ln* = La, Ce) (Fig. 7). The antibacterial investigation of Schiff bases and their Ln(III) compounds were completed against two *G(+)* (*SA*-ATCC25923, *LM*-ATCC19115) and two *G(-)* (*EC*-ATCC25922, *PA*-ATCC27583) bacterial strains by using micro-broth dilution assays,<sup>112,113</sup> with ciprofloxacin as standard drug. These complexes showed more activity against *G(+)* as compare to against *G(-)* which is due to outer membrane act like permeability barriers that holds the compound not reach at the targets.<sup>114</sup> La(III) complex of *L*<sub>22</sub> ligand with MIC<sub>125</sub> μg mL<sup>-1</sup> showed highest activity as compare to all other complexes. The current investigation concludes that bacteriostatic effect of free Schiff bases increases upon complexation with Ln(III) ions.

Mahmoud and co-workers (2020)<sup>115</sup> synthesized another ligand *H*<sub>2</sub>*L*<sub>26</sub>, through the condensation reaction of dibenzoylmethane with anthranilic acid and their three Ln(III) complexes of composition  $[\text{Ln}(\text{L}_{26})(\text{H}_2\text{O})(\text{NO}_3)]\text{H}_2\text{O}$  (*Ln* = Gd, Pr). The six coordination of Ln(III) ions obeyed by two nitrogen, two oxygen atoms from *L*<sub>26</sub>, one oxygen atom from water molecule and one oxygen from one nitrate ion (Fig. 5d). The antibacterial investigation was measured against two *G(+)* (*SA*, *BS*) and two *G(-)* (*ST*, *EC*) pathogens employing disc diffusion method.<sup>99</sup> The activity of Schiff base *H*<sub>2</sub>*L*<sub>26</sub> and its Gd(III) and Pr(III) complexes was evaluated using DMSO as solvent, with results expressed as inhibition zone diameters (mm). The free ligand exhibited inhibition zones of 10–16 mm, while the Gd(III) and Pr(III) complexes showed slightly enhanced activity with inhibition zones of 13–15 mm and 12–14 mm, respectively. The authors concluded that both complexes displayed greater potency against *G(-)* bacteria, whereas their activity against *G(+)* bacteria was slightly lower compared to the free ligand *H*<sub>2</sub>*L*<sub>26</sub>.

Taha *et al.* (2020)<sup>116</sup> published an article dealing with the synthesis ligand, *H*<sub>2</sub>*L*<sub>27</sub> through the condensation reaction of picolinoylhydrazide and salicylaldehyde in EtOH and their six lanthanide(III) complexes of the general formula  $[\text{Ln}(\text{H}_2\text{L}_{27})_2(-\text{NO}_3)_2]\text{NO}_3$  (*Ln* = La, Sm, Eu, Gd, Tb, Dy). The coordination number of Ln(III) ions in their complexes is ten involving four oxygen, two nitrogen atoms from *L*<sub>27</sub>, four oxygen atoms from two bidentate nitrate ions as shown in Fig. 4b. The antibacterial activities were evaluated against three *G(-)* (*SE*, *KP*, *EC*) and three *G(+)* (*SA*, *MRSA*, *EF*) bacterial strains using broth-dilution technique (MIC) with oxytetracycline as standard drug. The results showed that Ln(III) complexes exhibited more activity against *G(-)* bacteria than *G(+)* bacteria and authors concluded that the activity of Schiff base enhance upon complexes with Ln(III) ions which is comparable with the activity of standard drug oxytetracycline.

In another study, Paswan *et al.* (2020)<sup>117</sup> prepared two Schiff bases, *H*<sub>2</sub>*L*<sub>28</sub> and *H*<sub>2</sub>*L*<sub>29</sub> through the condensation reaction *o*-vanillin and 2-hydroxy-1-naphthaldehyde, respectively with



diethylenetriamine (DETA) and their six lanthanide(III) complexes of compositions  $[\text{Ln}(\text{NO}_3)_2(\text{H}_2\text{L}_{28})]\text{NO}_3 \cdot x\text{CHCl}_3 \cdot n\text{H}_2\text{O}$  and  $[\text{Ln}(\text{NO}_3)_2(\text{H}_2\text{L}_{29})]\text{NO}_3 \cdot x\text{CHCl}_3$  ( $\text{Ln} = \text{Nd}, \text{Yb}, \text{Dy}$ ). The reported coordination number of lanthanide ions was as eight occupied by two nitrogen, two oxygen atoms from ligands and four oxygen atoms from two bidentate nitrate ions as depicted in Fig. 2i and 6a. The activity of lanthanide nitrate salts, Schiff bases and lanthanide complexes were investigated against two G(−) (*EC*, *ST*) and two G(+) (*SA*, *EF*) bacterial strains by agar disc diffusion method; diameter of zone of inhibition and micro-broth dilution method; MIC.<sup>118</sup> The antibacterial evaluation of Schiff bases  $\text{H}_2\text{L}_{28}$ ,  $\text{H}_2\text{L}_{29}$  and their Ln(III) complexes revealed selective activity against both G(−) and G(+) strains. The Yb(III) and Dy(III) complexes of  $\text{H}_2\text{L}_{28}$  exhibited notable inhibition against *ST*, with inhibition zones of 17 and 18 mm and MIC values of >500 and 500  $\mu\text{g mL}^{-1}$ , respectively. In contrast, Nd(III) and Dy(III) complexes with  $\text{H}_2\text{L}_{29}$  demonstrated enhanced activity against *EF* and *SA*, showing inhibition zones of 16 mm and MIC values <500  $\mu\text{g mL}^{-1}$ . These findings suggest that Dy(III) complexes, in particular, display broad antibacterial

potential across multiple strains, with activity surpassing the corresponding free Schiff bases.

In another study (2020), a bidentate ligand ( $\text{HL}_{30}$ ) produced by the reaction of sulfanilamide and 2-hydroxy-1-naphthaldehyde and utilized for the synthesis of six lanthanide complexes having composition  $[\text{Ln}(\text{NO}_3)_2(\text{L}_{30})(\text{H}_2\text{O})_2]n\text{H}_2\text{O}$  ( $\text{Ln} = \text{Nd}, \text{Dy}, \text{Tb}, \text{Eu}, \text{Yb}$ ).<sup>119</sup> The coordination number of lanthanide ions in their metal complexes is eight by one nitrogen atom, one oxygen atom from  $\text{HL}_{30}$ , four oxygen atoms from two bidentate nitrate ions and two oxygen atoms from two aqua molecules (Fig. 6b). The antibacterial activity of ligand and its lanthanide complexes was assessed against *EC*, *SA*, *KP*, *AB*, *PA* strains using micro-broth dilution method (MICs) with levofloxacin as reference drug. The free ligand showed only moderate activity against *SA*, *KP*, and *PA* (MIC 32  $\mu\text{g mL}^{-1}$ ) and no effect on *EC* or *AB* (MIC > 64  $\mu\text{g mL}^{-1}$ ). Among the complexes, Dy(III) and Tb(III) displayed the most potent effects against *SA* (MIC 16  $\mu\text{g mL}^{-1}$ ), while Dy(III) also exhibited moderate inhibition of *EC*, *AB*, and *PA* (MIC 32  $\mu\text{g mL}^{-1}$ ). Tb(III) showed weaker activity against *PA* and no effect on *EC*, *KP*, or *AB*, whereas Eu(III)

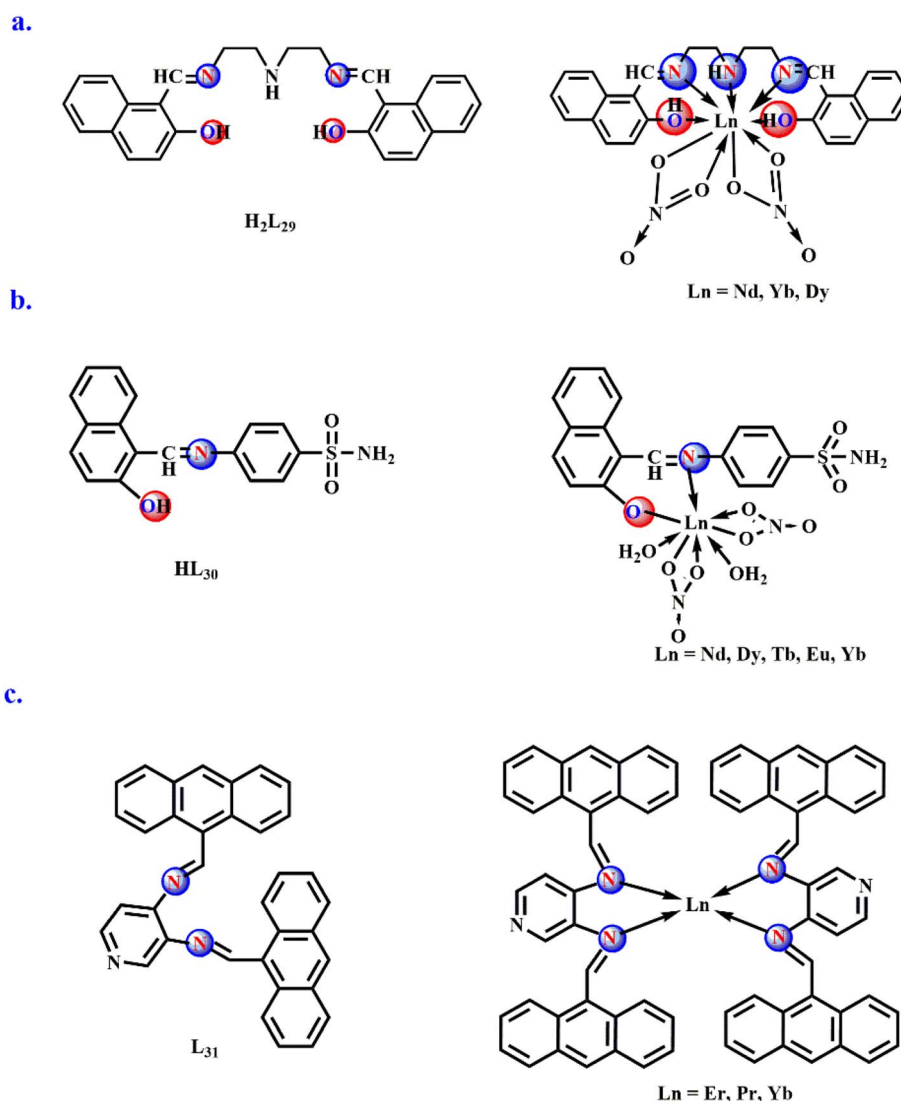


Fig. 6 Structure of Schiff base ligands and their Ln(III) complexes (a–c).



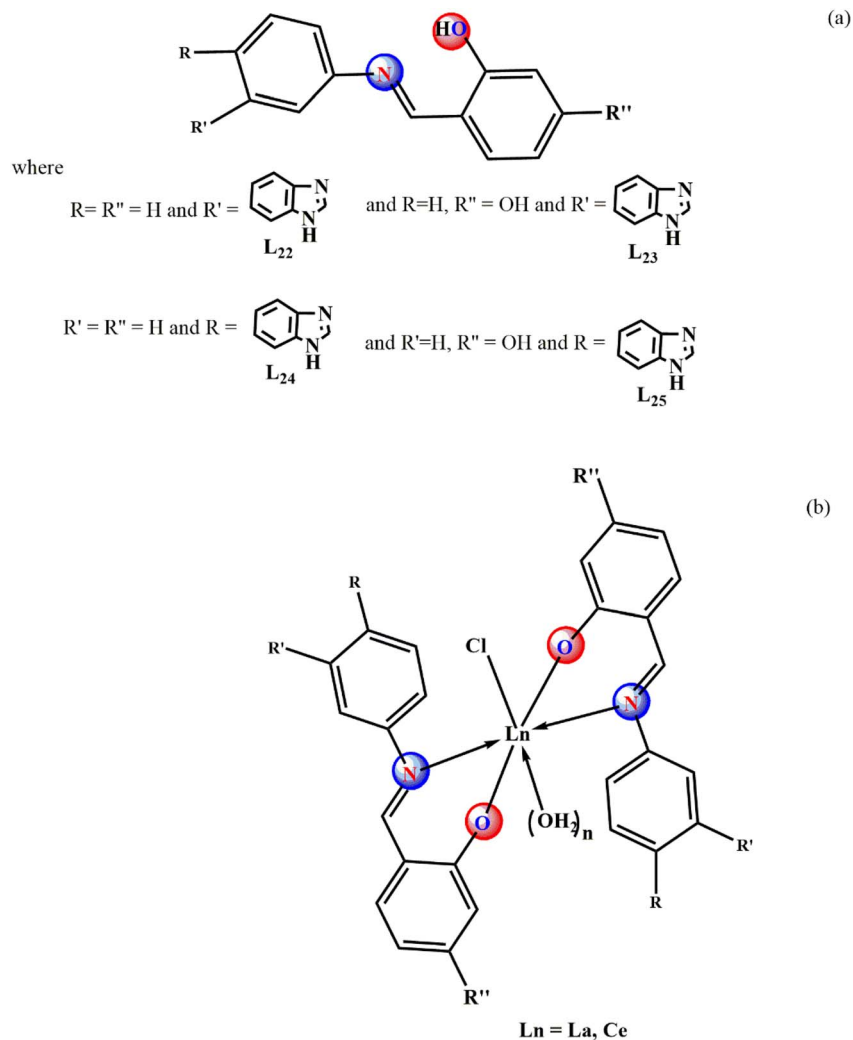


Fig. 7 Structure of (a) Schiff base ligands (HL22–25) and their (b) Ln(III) complexes.

displayed minimal activity limited to *SA*. Although less effective than the reference drug levofloxacin, these results highlight Dy(III) and Tb(III) complexes as the most promising candidates, particularly against *SA*.

Andiappan *et al.* (2019)<sup>76,120</sup> prepared Schiff base ( $L_{31}$ ) by the condensation reaction between 3,4-diaminopyridine and 9-anthraldehyde in MeOH and its three new lanthanide complexes of composition  $[Ln(L_{31})_2]$  ( $Ln = Er, Pr, Yb$ ) (Fig. 6c). These complexes were screened for antibacterial activity against G(+) (*SA, BS*) and G(−) (*PA, EC*) strains using well diffusion and micro dilution method and results expressed in term of size of inhibition zones and in MICs values with gentamycin as standard drug. The Er(III) complex demonstrated strong inhibition against *EC* and *BS*, but only weak activity toward *SA* and *PA*. A concentration-dependent enhancement of antibacterial activity was observed, with higher doses leading to larger inhibition zones. The Pr(III) complex showed the most pronounced effects, yielding inhibition zones of 20 mm (*BS*), 17 mm (*SA*), 20 mm (*EC*), and 23 mm (*PA*) at  $100 \mu\text{g mL}^{-1}$ . Moreover, all the complexes displayed low MIC values, confirming their

promising antibacterial potential. Among them, the Pr(III) complex exhibited the strongest activity, correlating with its broader inhibition spectrum and lower MIC values. Overall, all the synthesized lanthanide Schiff base complexes were effective against the tested bacterial pathogens.

Mosquera and collaborators (2018)<sup>121</sup> described the synthesis of two Schiff base ligands, HL<sub>32</sub> HL<sub>33</sub> and its six novel lanthanide complexes having compositions  $[Ln(L_{32})_2(Cl)] \cdot nH_2O$  and  $[Ln(L_{33})_2(Cl)] \cdot nH_2O$  ( $Ln = La, Nd, Eu$ ). The stoichiometric ratio of metal to ligand in all the synthesized complexes is 1 : 2. The coordination number of lanthanide ions in their complexes is nine involving two nitrogen atoms, two sulphur atoms, four oxygen atoms from Schiff bases and from one chlorido ligand as shown in Fig. 4c and d. The antibacterial activity of ligands and its lanthanide complexes were evaluated by micro-dilution technique in term of MIC against one G(+) bacteria (*SA-ATCC25923*) and four G(−) bacteria (*EC-ATCC25922, ST-ATCC14028, KP-ATCC2146, KP-ATCC1705*).<sup>112</sup> The results demonstrated that all lanthanide–Schiff base complexes exhibited comparatively lower antibacterial activity against G(−)



strains, while showing enhanced activity against G(+) strains, particularly *SA*. Notably, the Eu(III) complex displayed the strongest effect with a MIC value of 63  $\mu\text{g mL}^{-1}$ . These findings highlight that coordination with lanthanide ions significantly improves the antibacterial potency of Schiff base ligands, likely due to increased lipophilicity and facilitated penetration of the bacterial cell wall.

Ajlouni *et al.* (2018)<sup>122,123</sup> synthesized Schiff base (HL<sub>34</sub>), *via* condensation of furan-2-carbaldehyde with 2-fluorobenzohydrazide and its eight lanthanide complexes with the general formula [Ln(L<sub>34</sub>)<sub>2</sub>(NO<sub>3</sub>)<sub>2</sub>]NO<sub>3</sub> (Ln = La, Pr, Nd, Sm, Eu, Gd, Dy, Er). The complexes exhibited a 1:2 metal-to-ligand stoichiometry, with the Ln(III) ions attaining a coordination number of ten through interactions with two nitrogen atoms, four oxygen atoms from HL<sub>34</sub>, and four oxygen atoms from two bidentate nitrate ligands (Fig. 4e). Antibacterial activity, evaluated by the agar well diffusion method, revealed weak to negligible effects against G(+) (*SA*, *SPy*, *EF*), but comparatively higher activity against G(−) (*EC*, *KP*, *PM*, *SE*, *PA*) bacterial strains. *PM* and *SE* were the most susceptible, with MIC values ranging from 16–250  $\mu\text{g mL}^{-1}$ , while *EC* and *KP* were also inhibited within the same range. Among G(+) strains, *SPy* showed moderate susceptibility to five complexes (MIC 125–250  $\mu\text{g mL}^{-1}$ ). Overall, the activity of the ligand and its complexes was significantly lower than that of the reference drug oxytetracycline. The authors concluded that Ln(III)–hydrazone complexes act as selective inhibitors of G(−) pathogens, likely due to their interaction with structural features of the bacterial cell wall.<sup>124a</sup>

We have observed that most of synthesized Schiff bases generally contain both N and O donor atoms, to avoid dechelation they prepared in the absence of water. The hard Lewis acid nature of Ln(III) ions enables this ions that they preferentially coordinate oxygen donors, whereas Schiff bases primarily bind through azomethine nitrogen atoms. Consequently, many Ln–Schiff base complexes exhibit comparatively weaker metal–ligand interactions than oxygen-rich chelators, making them susceptible to dechelation and hydrolytic ligand exchange, particularly in aqueous and biologically relevant environments.<sup>124b,c</sup> Recent potentiometric studies on Eu(III), Gd(III), and Tb(III) complexes with salicylidene-based Schiff bases demonstrate the formation of hydrolysed species, Ln–SB(OH)<sub>x</sub>, at higher pH, highlighting partial disruption of the coordination sphere.<sup>124d</sup> Such instability has direct implications for luminescent applications, as partial ligand dissociation allows water coordination, which quenches lanthanide-centered emission through O–H vibrational relaxation. Dechelation also plays a pivotal role in biological systems. Schiff base complexes of Ln(III) ions may release aqua Ln(III) ions in solution, which readily interact with biomolecules such as amino acids, nucleotides, and phosphate-containing metabolites due to the ions' high kinetic lability.<sup>124e,f</sup> Amino acids like aspartate, glutamate, cysteine, and histidine, as well as nucleotide phosphates, can displace coordinated water to form Ln(III)–biomolecular adducts, leading to dynamic speciation in physiological conditions. This competitive coordination can modulate metal ion uptake, enzymatic activity, and nucleic acid interactions, while

also facilitating metal-mediated oxidative stress or catalytic processes.<sup>124g</sup> Importantly, dechelation is not an inherent limitation of all Schiff base systems. Modern ligand designs incorporating phenolate oxygen donors, increased denticity, rigid backbones, and mixed N,O-donor sets significantly improve thermodynamic stability and kinetic inertness.<sup>124d,h</sup> Mixed-ligand complexes, such as those combining Schiff bases with strong  $\beta$ -diketonate co-ligands, demonstrate robust structural integrity in solution and preserve luminescence, underscoring the critical role of ligand design in mitigating dechelation. Overall, the biological activity and solution behavior of Ln(III) ions are intimately connected to their kinetic lability and coordination environment. In both Schiff base complexes and biological media, Ln(III) ions predominantly exist as dynamic aqua or biomolecularly coordinated species. Their interactions with amino acids, nucleotides, and other biomolecules govern their luminescence, pharmacological activity, and potential toxicity. Therefore, consideration of both dechelation and biomolecular adduct formation is essential for evaluating the functional and biological implications of lanthanide complexes.

The majority of reported lanthanide–Schiff base complexes exhibit good solubility in polar aprotic solvents such as DMSO and DMF, limited solubility in alcohols and moderately polar organic solvents, and negligible solubility in non-polar media and water.<sup>107,110,122–124a</sup> These solvent-dependent solubility trends are consistent with their ionic and coordination-driven structures. Representative examples reported by Taha *et al.*<sup>90</sup> further confirm that such complexes are air-stable, non-hygroscopic, and remain intact in solution. The solution stability is corroborated by well-defined UV-Vis spectral signatures and the consistent enhancement of antibacterial activity relative to the free Schiff bases. The clear differences in spectroscopic profiles and MIC values between ligands and their corresponding complexes strongly support the persistence of intact metal–ligand coordination in solution, which is essential for reliable biological evaluation. The limited solubility of these complexes in common solvent may also indicate the presence of aggregate or nanoparticulate species, which could contribute into the biological activity.

### 3.1 Characterization techniques for lanthanide complexes

A comprehensive characterization is essential for establishing the structure, purity, and stability of Schiff base lanthanide complexes prior to evaluating their biological properties. A set of complementary tools are required to characterize lanthanide complexes due to their high coordination numbers and flexible geometries.

Fourier transform infrared (FT-IR) spectroscopy is typically the first line of evidence for metal coordination. Upon chelation, the azomethine HC=N stretching band (usually 1610–1640  $\text{cm}^{-1}$ ) undergoes a characteristic shift to lower wavenumbers, indicating donation of electron density from the imine nitrogen to Ln(III) ions.<sup>54,57,70,74,85,90</sup> Concurrently, disappearance or broadening of phenolic O–H stretching signals in lanthanide complexes compare to ligands confirms



deprotonation and O-coordination.<sup>57,107</sup> Shifts in C–O, C=N, and sometimes N–N vibrations provide additional diagnostic information and help differentiate mono-, bi-, or tridentate binding modes.<sup>107</sup>

Elemental analysis (CHN) and high-resolution ESI mass spectrometry (HR-MS) provide indispensable confirmation of stoichiometry, purity, and the presence of intact complex ions. HR-MS often reveals ligand-loss fragments or solvated species, allowing insight into solution speciation—especially important for Ln(III) complexes with labile coordination spheres.<sup>83</sup>

Single-crystal X-ray diffraction remains the authoritative method for elucidating coordination geometry, structural topology, and ligand denticity around Ln(III) centre. Due to the large ionic radii and flexible coordination environments, diffraction often reveals 7–10 coordination numbers, distorted polyhedral geometries, and intramolecular or intermolecular hydrogen-bond networks that influence solution stability and biological function.<sup>74</sup> Lanthanide contraction trends, such as decreasing Ln–O/N bond distances across the series, have been extensively documented using crystallographic data.<sup>24</sup> Thus, even a small number of representative ORTEP structures significantly strengthen structural arguments in any investigation.

UV-Vis absorption spectroscopy is widely used to monitor ligand centered ( $\pi$ – $\pi^*$ ,  $n$ – $\pi^*$ ) transitions and ligand-to-metal charge transfer (LMCT) bands. Time-dependent UV-Vis measurements also allow qualitative assessment of solution stability under physiological pH ranges. For many Schiff base ligands, dramatic spectral differences upon complexation with metal ions serve as additional evidence for chelation. Electronic transitions in the 4f orbitals of lanthanide ions give rise to characteristic absorption spectra. Only  $Y^{3+}$ ,  $La^{3+}$  and  $Lu^{3+}$  do not absorb in the UV or visible domain; all the other lanthanides have characteristic bands in this region, but the absorptivities have low values. The literature indicates that Schiff bases typically display two major absorption peaks: one below 300 nm attributed to  $\pi$ – $\pi^*$  transitions and another between 300–450 nm corresponding to  $n$ – $\pi^*$  transitions. Upon complexation with Ln(III) ions, these bands shift, confirming coordination between the ligand and the metal center. Additionally, the Ln(III) complexes exhibit new absorption features in the 410–475 nm range, which are absent in the free ligands. These newly appeared bands are assigned to intra-ligand charge-transfer transitions, consistent with quantum-chemical calculations.<sup>54,57,66,70,74,83</sup>

Lanthanide ions such as Sm(III), Eu(III), Tb(III), and Dy(III) exhibit strong characteristic luminescence because their accepting 4f excited states lie slightly below the excited energy levels of coordinated ligands, enabling efficient ligand-to-metal energy transfer (LMET). Detectable luminescence is typically achieved upon excitation by ultraviolet light, X-rays, or other high-energy stimuli. Complexation with suitable chromophoric ligands markedly enhances lanthanide emission through the well-known antenna effect, in which the ligand absorbs energy and transfers it non-radiatively to the metal center. Luminescence spectroscopy is therefore a powerful tool for probing Eu(III), Tb(III), Dy(III) and Sm(III) complexes. Schiff base ligands

commonly act as effective sensitizers in these systems, and photophysical parameters such as emission intensity, excitation profiles, and excited-state lifetimes provide critical information on energy-transfer efficiency, coordination environment, and dominant quenching pathways. Numerous studies have demonstrated that Sm(III) and Tb(III) Schiff base complexes display intense, metal-centered emissions, confirming efficient ligand-sensitized energy transfer, whereas in some Eu(III) and Gd(III) systems weak or ligand-based emission indicates inefficient antenna behaviour.<sup>40b,57,124a,b</sup>

Magnetic susceptibility measurements and electron paramagnetic resonance (EPR) are valuable for paramagnetic lanthanides such as Gd(III), Dy(III), and Tb(III). These techniques provide insight into electronic environments, spin-orbit coupling, and coordination anisotropy. Although less frequently reported than IR or UV-Vis spectroscopy, magnetic data enhance understanding of structure–property relationships, particularly in mixed-metal or high-spin systems. Alquasimeh *et al.*<sup>74</sup> measured magnetic moment of Nd, Tb, Dy complexes with HL<sub>8</sub> Schiff base by measuring magnetic susceptibility by the Curie–Weiss (C–W) law:

$$\chi_T = \chi_{\text{dia}} + C/T - T_{\text{CW}}$$

where  $\chi_{\text{dia}}$  is the diamagnetic contribution,  $C$  is the Curie constant and  $T_{\text{CW}}$  the Curie–Weiss temperature. The experimental data indicates weak antiferromagnetic interactions for complexes with Nd(III) and with Dy(III) and antiferromagnetic interactions of the complex with Tb(III). The Curie constant was used to determine the effective magnetic moment. The values of the effective magnetic moments of the Nd(III) ( $\mu_{\text{eff}} = 3.60\mu_B$ ), Tb(III) ( $\mu_{\text{eff}} = 9.61\mu_B$ ) and Dy(III) ( $\mu_{\text{eff}} = 10.61\mu_B$ ) ions correspond to the theoretical values of magnetic moments  $\mu_{\text{th}} = 3.62, 9.72, 10.63\mu_B$ , respectively. The slight differences in the theoretical and effective values of the moments are due to antiferromagnetic interactions between the magnetic ions.<sup>74</sup> The mixed ligands La(III), Er(III) and Yb(III) complexes were reported as diamagnetic.<sup>83</sup> From the effective magnetic moment ( $\mu_{\text{eff}}$ ) values the Nd(III), Gd(III), Er(III), Dy(III) complexes of L<sub>19</sub> Schiff base were found as paramagnetic.<sup>100</sup>

Together, these characterization techniques ensure that Schiff base lanthanide complexes are structurally well-defined, chemically pure, and stable under relevant conditions.

## 4. Mechanistic insights and structure–activity relationships (SAR)

### 4.1 Structure–activity relationships (SAR)

An analysis of antibacterial studies published between 2018 and 2025 indicates that Schiff bases and their Ln(III) complexes may be broadly classified into three categories of activity: highly active, moderately active and weakly active agents. Ligands such as L<sub>7</sub>, H<sub>2</sub>L<sub>13–14</sub>, and H<sub>2</sub>L<sub>20</sub>, along with their Ln(III) complexes displayed the most promising activity with MIC values of 2–64  $\mu\text{g mL}^{-1}$  and inhibition zones  $\geq 20$  mm, particularly against SA, EF, MRSA, KP, SE, and EC. By contrast, ligands including L<sub>4</sub>, L<sub>12</sub>, L<sub>15–16</sub>, HL<sub>30</sub>, HL<sub>32–34</sub> and their complexes were only moderately



active, with MICs of 64–195  $\mu\text{g mL}^{-1}$  and inhibition zones of 10–20 mm, mainly effective against *SA*, *BS*, and *EC*. Finally, Schiff bases such as  $\text{H}_2\text{L}_{6-6}$ ,  $\text{L}_{22-25}$ ,  $\text{H}_2\text{L}_{27}$  and their corresponding complexes exhibited weak or negligible antibacterial activity ( $\text{MIC} > 195 \mu\text{g mL}^{-1}$ ; inhibition zones  $< 10 \text{ mm}$ ), showing limited effectiveness against most bacterial strains (Fig. 12). Among the studied compounds,  $\text{La(III)}$ ,  $\text{Nd(III)}$ ,  $\text{Gd(III)}$  and  $\text{Dy(III)}$  complexes with highly active tridentate and tetradentate Schiff bases ( $\text{L}_7$ ,  $\text{H}_2\text{L}_{13-14}$ ,  $\text{L}_{20}$ ), incorporating electron-withdrawing substituents such as Cl, Br, and  $-\text{NO}_2$ , were found to possess coordination numbers of 7–9 along with their notable antibacterial activities, as reflected by MIC values and inhibition zone diameters, are summarized in Schemes 2–5. These observations emphasize that ligand substituents, donor atom sets (N, O, S), and coordination numbers (6–9) play key roles in modulating activity. The halogen and heteroatom-substituted Schiff bases generally enhancing antibacterial potency. The biological activity consistently follows the trend: free Schiff base  $<$   $\text{Ln(III)}$ –Schiff base complex  $<$  conventional antibiotics—although, top-performing  $\text{Ln(III)}$  complexes occasionally approach standard drug efficacy. These structure–activity insights underscore the importance of both the identity of the lanthanide ion and the coordination environment in determining antibacterial potency.

#### 4.2 Mechanistic insights

An antimicrobial agent is a compound that can kill bacteria by binding to essential metabolic components and preventing the formation of functioning biomolecules, which interferes with normal cellular functions.<sup>125</sup> The antibacterial activity of drugs is primarily achieved through two strategies, which entail interfering chemically with the synthesis or functioning of crucial bacterial components and/or dodging known antibacterial resistance mechanism. The bacterial cell contains many targets for antibacterial drugs that include (a) bacterial protein biosynthesis (b) bacterial cell-wall biosynthesis (c) bacterial cell membrane destruction (d) bacterial DNA replication and repair, and (e) inhibition of a metabolic pathway.<sup>126</sup> It is very crucial to find a solution for antibacterial resistance mechanisms because bacteria can exhibit resistance through a variety of mechanisms, which primarily include activating the efflux pumps, destroying antibacterial agents with the help of destruction enzymes, modifying antibiotics with the help of modifying

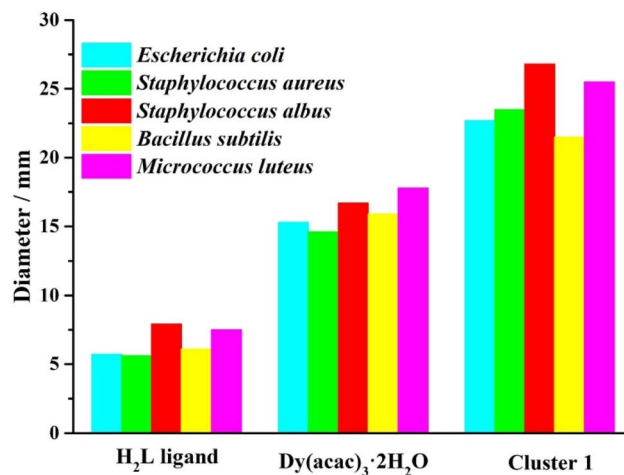


Fig. 9 Diameters of growth inhibition areas of ligand  $\text{H}_2\text{L}_5$ ,  $\text{Dy(acac)}_3 \cdot 2\text{H}_2\text{O}$  and  $\text{Dy(III)}$  cluster.

enzymes, and altering target structures in the bacterium that have lower affinities for an antibiotic.<sup>127</sup> Some types of antibiotics need metal ions to work properly. These metal ions can either be important to the structure of the antibiotic, and therefore their removal renders the antibiotic structure inactive, or bind to the antibiotic molecules and cause important chemical and biochemical reactions without changing the antibiotic structure.<sup>128</sup> The lanthanide complexes as antibacterial drugs have a benefit that  $\text{Ln}^{3+}$  and  $\text{Ca}^{2+}$  have similar ionic radii, the lanthanide ions have the potential to block calcium channels because of their greater charge and strong affinity for the  $\text{Ca}^{2+}$  sites on biological molecules. Thus, even though the lanthanide ions cannot get through cell membranes on their own, they can still affect calcium channel's external face by blocking them. The lanthanides have the potential to substitute for the calcium in proteins, which can either inhibit or significantly enhance the activity of calcium-dependent enzymes.<sup>25</sup> The higher antibacterial activity of metal complexes can be explained on the basis of two theories that comprise (i) Tweedy's chelation theory<sup>129</sup> (ii) Overtone's concept.<sup>130</sup> The presence of the imine ( $-\text{C}=\text{N}$ ) group in the Schiff base ligands, which provides them their biological activity, facilitated the rationalisation the antibacterial activity and offered a mechanism of transamination and resamination reactions in biological

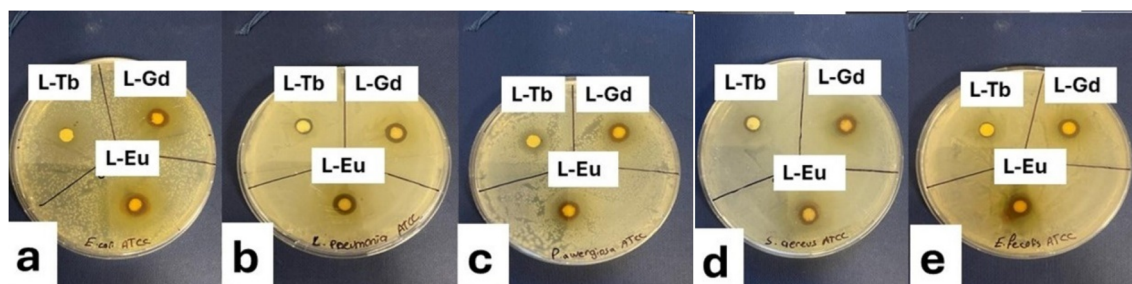


Fig. 8 Agar disc diffusion assay results of  $\text{Eu(III)}$ ,  $\text{Tb(III)}$  and  $\text{Gd(III)}$  complexes of  $\text{H}_2\text{L}_1$  ligand against (a) *EC*, (b) *KP*, (c) *PA*, (d) *SA*, (e) *EF*, bacterial strains.



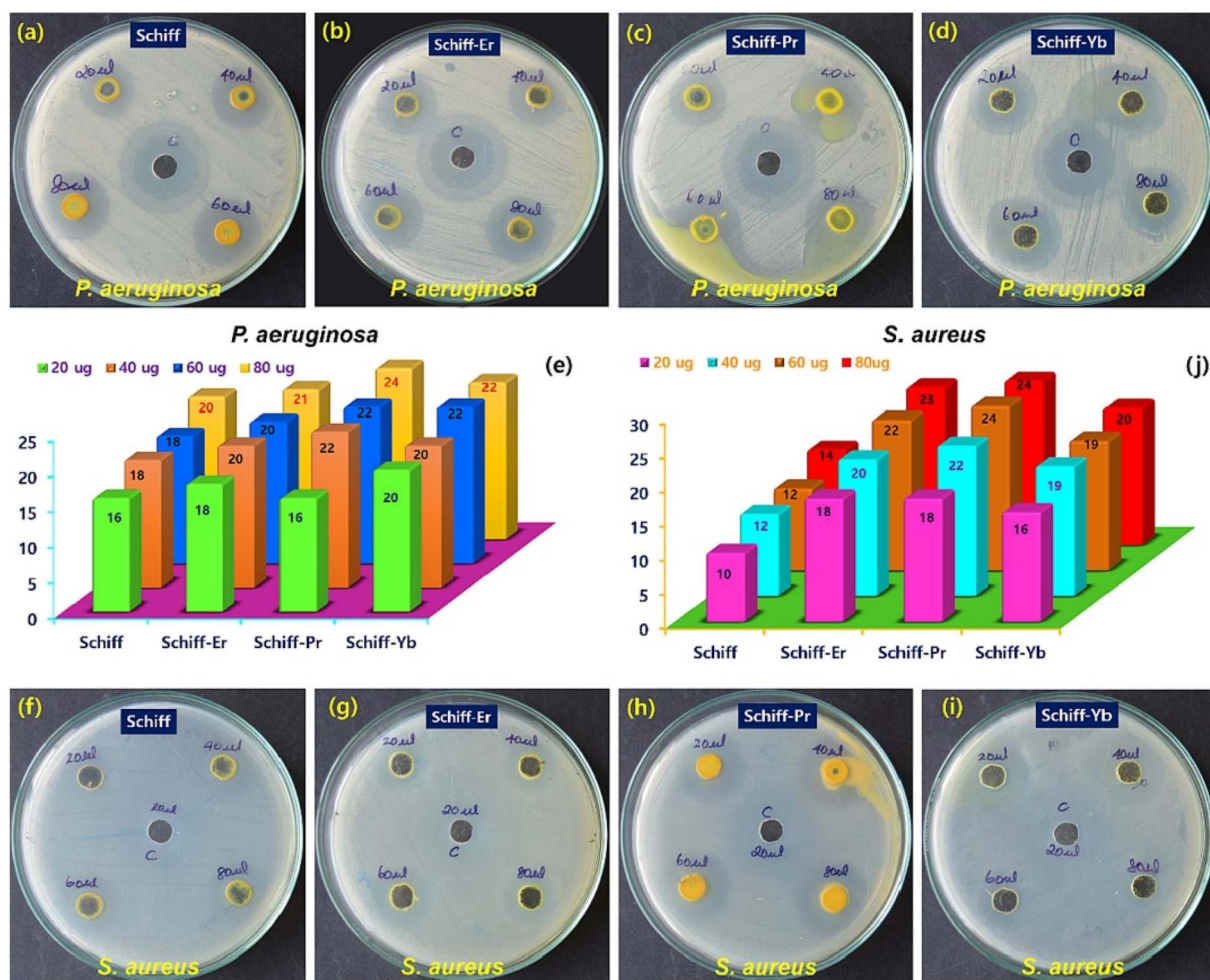


Fig. 10 The diameters of zone of inhibition of  $L_9$  ligand and its  $Ln(III)$  (Er, Pr, Yb) complexes against *PA* and *SA* strains at various concentrations 20, 40, 60, 80  $\mu\text{g mL}^{-1}$ .

systems work.<sup>121,124,131,132</sup> The ligands have demonstrated to form hydrogen bonds with bacterial strain through azomethine moiety, thereby resulting in enhanced cell inhibition. Furthermore, it has been hypothesised that Schiff bases with nitrogen, oxygen and sulphur donor atoms may also be capable of inhibiting bacterial cell growth.<sup>133–135</sup> According to extant literature in the preceding discussion; most research has demonstrated that lanthanide complexes with Schiff bases exhibit higher activity than free Schiff bases and metal salts. This enhancement in activity can be attributed to the increased chelation exhibited by lanthanide complexes, a phenomenon that may be explained by Tweedy's chelation theory. This theory facilitates the delocalization of  $\pi$ -electrons across the whole chelate ring; resulting the positive charge on the metal ions is reduced and an enhancement of the lipophilicity of the metal chelate, favouring its permeation across the lipid barrier inside bacterial membranes.<sup>136,137</sup> According to Overtone's concept of cell permeability, the lipid membrane that envelops the cell selectively permits the passage of lipid-soluble compounds; resulting liposolubility has been identified as a crucial variable

that regulates antimicrobial action. It has been established that the overlap of the ligand orbital and the partial sharing of the positive charge of the metal ion with donor groups during chelation result in a lowering of the polarity of the metal ion. This, in turn, favours the lipophilicity of metal complexes. As the lipophilicity of the complexes increases, there is concomitant increase in penetration of the complexes through the lipid membranes of the cell. This is due to the metal binding sites in the bacterial enzymes being blocked, which in turn causes disturbance to the normal functioning of the cell. While moderate lipophilicity facilitates membrane penetration and enhances antimicrobial potency, excessive hydrophobicity in lanthanide-Schiff base complexes can promote self-aggregation and nanoparticle formation, which significantly alters their biological behavior. Such nanostructures may interact with bacterial membranes *via* surface adhesion, membrane destabilization, and mechanical perturbation. Moreover, their cellular uptake pathways can differ substantially from those of discrete molecular chelates, thereby influencing the observed antibacterial activity.



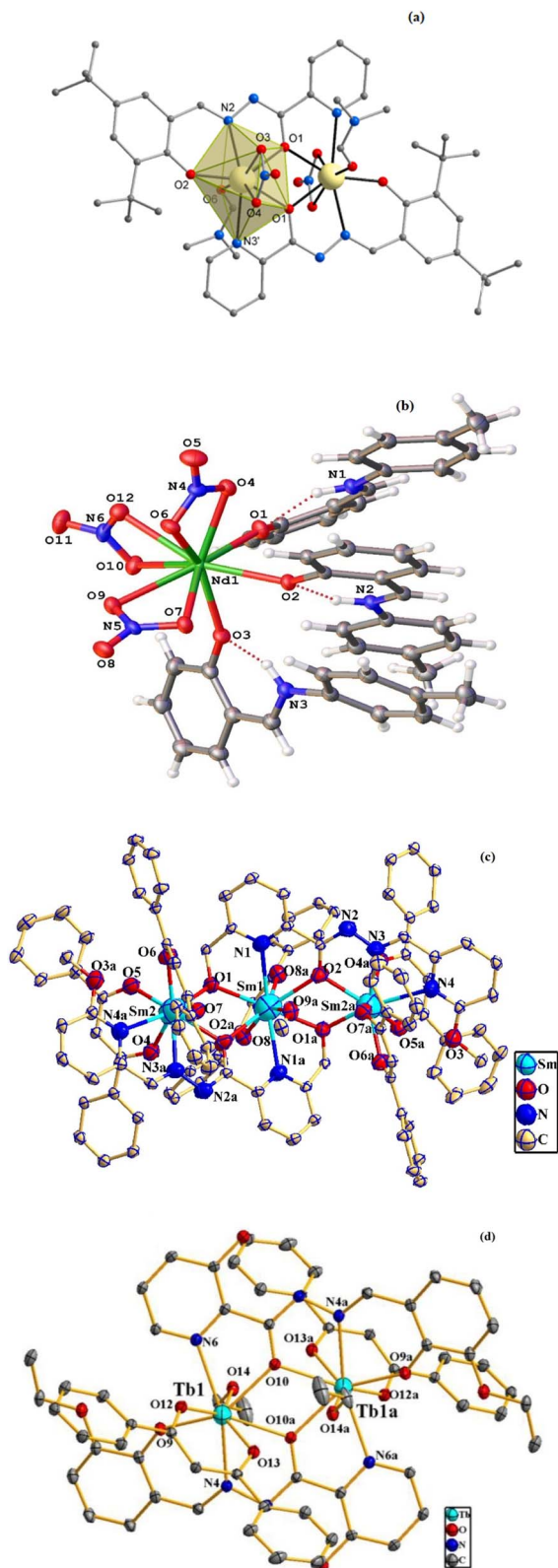


Fig. 11 The representative single-crystal structures (ORTEP diagrams) of the (a) Dy(III) complex with  $L_6$  ligand (b) Nd(III) complex with  $HL_8$  (c) Sm(III) complex with  $H_2L_{10}$  (d) Tb(III) complex with  $H_2L_{10}$  ligand.

## 5. Comparative analysis with previous reviews

Most of the earlier reviews on Schiff base and their Ln(III) complexes, largely published before 2020, mainly focused on synthetic strategies, structural characterization and general coordination chemistry with antibacterial application often mentioned only as a secondary aspect. For instance, Hameed *et al.* (2017)<sup>138</sup> presented a patent-based general overview of Schiff bases and their metal complexes, highlighting numerous therapeutic applications (2010–2015), including antibacterial effects. However, systematic quantitative comparisons, mechanistic insights, and detailed structure–activity relationships of antibacterial investigation were lacking. The review “*Metal complexes driven from Schiff bases and semicarbazones for biomedical and allied applications: a review*” by More *et al.* (2019)<sup>139</sup> examined a broad set of biological activities of Schiff base and its metal complexes, including antibacterial, but mostly focusing on transition metals, with fewer details for lanthanide systems. X. Leu and J. Hamon (2018),<sup>140</sup> provided a broad overview of synthesis and structure of multidentate Schiff bases and its coordination with transition and inner transition metal ions to form metal complexes with catalytic, magnetic and few biological applications, while K. Prajapati (2018)<sup>141</sup> highlighted several ligands and its Ln(III) complexes for antibacterial activities with general importance of these complexes in biological fields. In addition, Kaczmarek *et al.* (2018)<sup>33</sup> highlighted synthetic method, several structure of Schiff base and their Ln(III) complexes, role of these complexes in different biological fields such as cancer diagnosis, therapy and biological activity. I. Cota *et al.* (2019)<sup>2</sup> published a comprehensive review that extensively compiled studies on Ln(III) Schiff base complexes as antibacterial and anti-fungal agents, covering the period from 1995 to 2019. This review emphasizes interaction different Schiff bases and lanthanide complexes against both G(+) and G(–) bacterial strains, their antibacterial results and mechanistic interpretations. Another review, ‘*Advanced and Biomedical Applications of Schiff-Base Complexes and their metal complexes: A Review*’ (2022),<sup>142</sup> summarised recent work since about 2015, with some attention to anti-bacterial activity, but again the structure–activity relationships, coordination numbers, and systematic comparisons among Ln(III) ions were not thoroughly analysed. The work by Rakshit *et al.* (2023)<sup>143</sup> mainly provides antimicrobial behaviours, some techniques of antimicrobial measurement and structure of most of the transition metal complexes derived from only N, O donor ligands but it did not provide proper information about structure–activity relationships, mechanism for higher activity, classification of ligands and their metal complexes into different activity categories.

Unlike these prior works that emphasized synthesis, catalytic, photophysical or broad biological applications, our review mainly focused on data driven, mechanistic perspectives and structure–activity relationship (SAR) analysis of Schiff bases and their lanthanide complexes based on the 2018–2025 literature. Specifically, earlier reviews often lacked bulk of investigation on: (a) detailed MIC and inhibition zone data for different



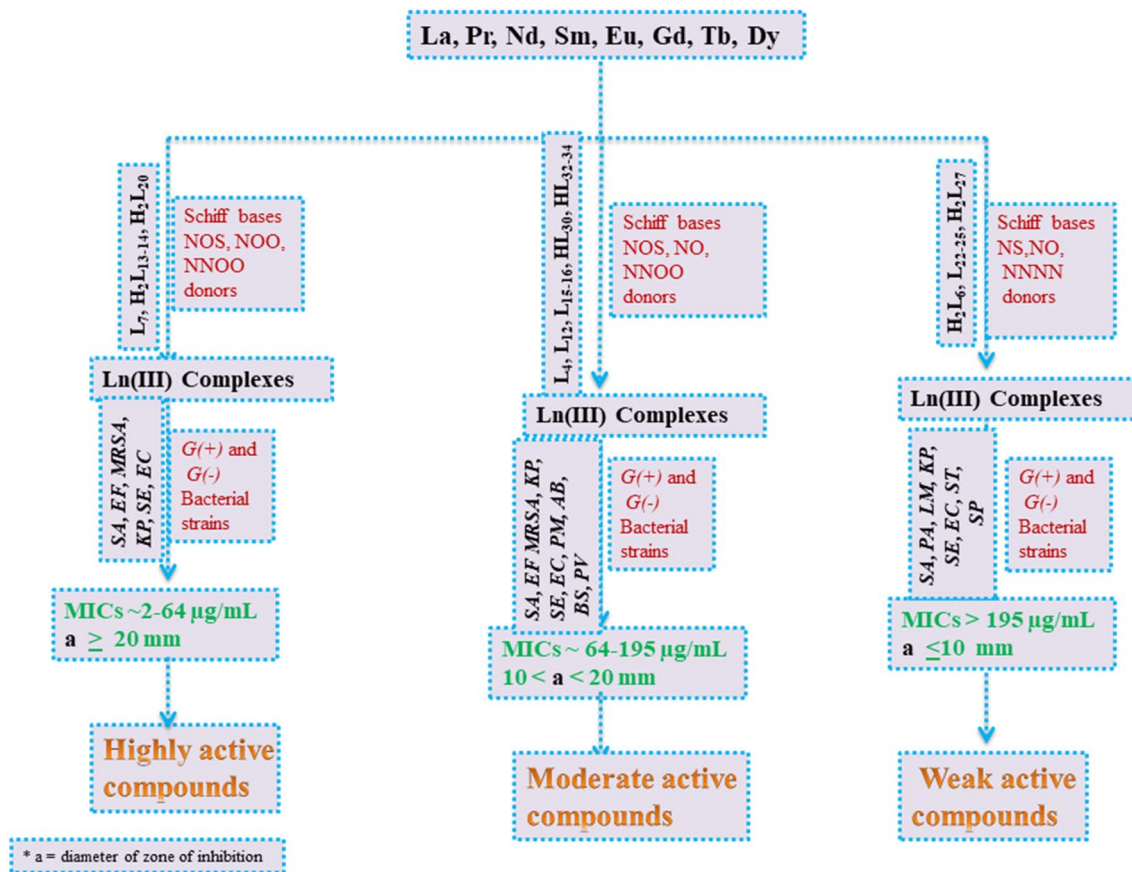


Fig. 12 General representation of antibacterial activity trends of Schiff base–lanthanide complexes (2018–2025), showing classification into highly active, moderately active, and weakly active compounds based on MIC values and inhibition zone diameters.

bacteria (b) comparisons of donor atom types, substituent effects (such as halogen or nitro groups) and coordination geometries (c) clear classification of compounds by potency (e.g. highly active vs. moderate vs. weak). By compiling recent studies, our review identifies clear trends: Schiff base ligands alone usually show modest or weak antibacterial activity, which is significantly enhanced upon complexation with lanthanides. We find that certain Ln(III) ions (La, Nd, Eu, Gd Dy) with ligand features (NOS donor sets, halogen and  $-\text{NO}_2$  substituents) correlate with higher potency. Moreover, our classification into highly, moderately, and weakly active agents as given in Fig. 12, provides a framework that was generally not present in previous reviews. We also tried to integrate mechanistic insights like enhanced lipophilicity, improved membrane permeability and enzyme inhibition. These mechanistic angles are systemically linked to structural parameters. Finally, our coverage includes direct comparisons of Ln–Schiff base complexes to standard antibiotics (in many 2018–2025 studies) in terms of MIC and inhibition zones, which few prior reviews addressed in detail.

In conclusion, while previous reviews laid the foundational understanding of Schiff bases and their metal complexes, our review advances the field by offering a data-driven, mechanistically informed and structure–activity focused perspective of the most recent antibacterial findings (2018–2025), which can guide rational design of new compounds.

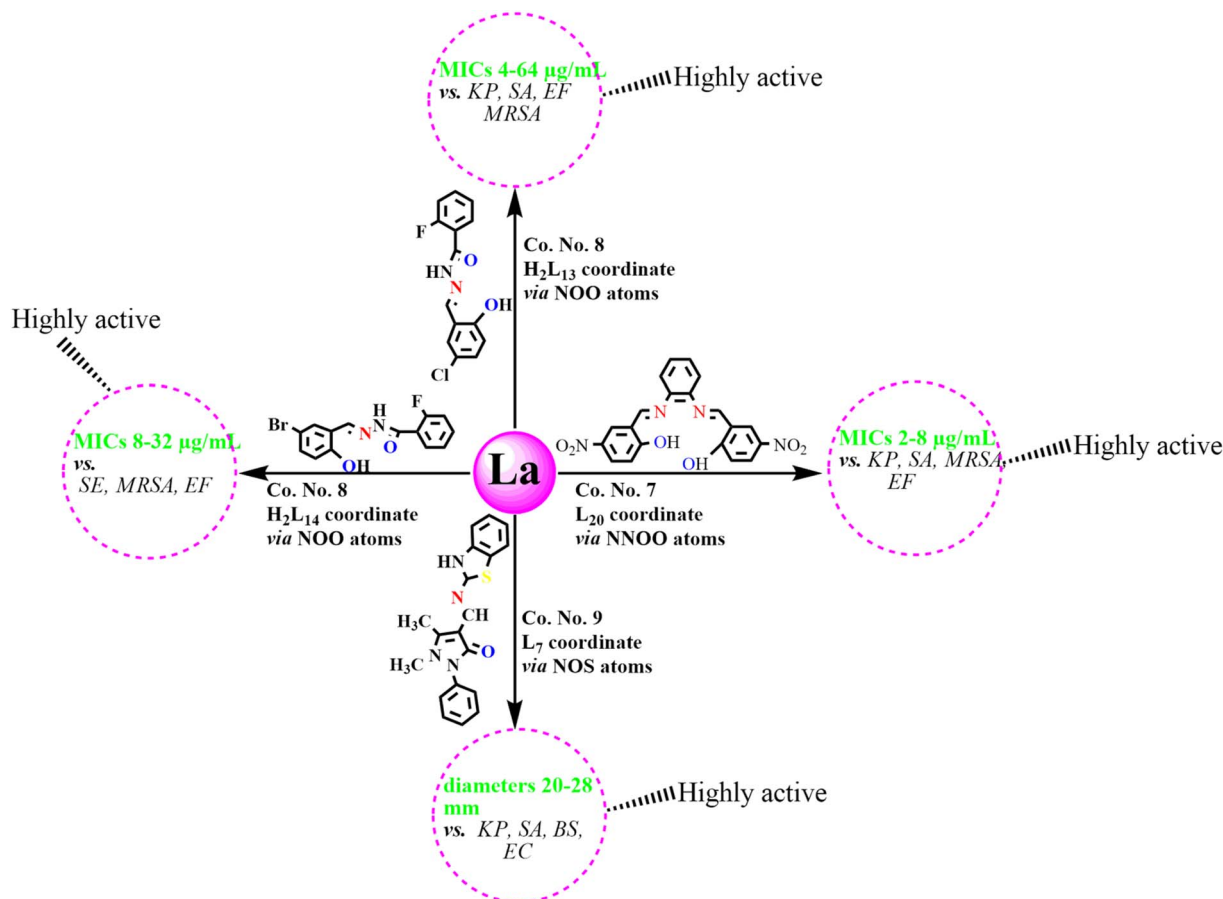
## 6. Techniques for evaluating antibacterial activity of complexes

Some of important techniques used for evaluating the antibacterial activity of chemical compounds.

### 6.1 Diffusion methods

**6.1.1 Agar disc-diffusion technique.** Agar disc diffusion technique was developed in 1940, and it is the certified method based on the principle that antibiotic-impregnated disc, which is employed on agar formerly inoculated with the test bacterium, pick-up moisture and the antibiotic diffuses easily outward through the agar medium generating an antibiotic concentration gradient.<sup>144</sup> It is widely used in various clinical microbiology laboratories to test antimicrobial susceptibility.<sup>12,145</sup> The size of the zone around each antibiotic disc reflects the lethality of that antibiotic against the microorganisms. However, this method is not universally accurate for all fastidious microbes, certain species like *streptococci*, *Haemophilus influenzae*, *Haemophilus parainfluenzae*, *Neisseria gonorrhoeae*, and *Neisseria meningitidis* have been successfully tested. This was achieved through standardization using tailored culture media, specialized incubation conditions, and clearly defined inhibition zone criteria.<sup>146</sup> While this method is not





Scheme 2 Most potent La(III)-Schiff base complexes against different bacterial strains.

suitable to find the minimum inhibitory concentration (MIC) value due to inability of quantify the drug diffusion in the agar medium, however an approximate MIC can still be calculated for some microbes and antibiotics by comparing the inhibition zones with stored algorithms.<sup>147</sup> However, the disc diffusion method has various advantages including its simplicity, low cost and its capability to test a wide range of various microorganism and antimicrobial agents, in addition to the evaluation of results.<sup>148</sup> The above-mentioned advantages can be attributed to the effective interconnection between the *in vitro* and *in vivo* evolution. This fact is given above mainly simplicity; low cost has contributed to its common use antimicrobial screening of pathogenic bacteria.<sup>149-151</sup>

**6.1.2 Agar well diffusion method.** This approach has been successfully employed to assess the antimicrobial properties of plants and microbial extracts.<sup>152,153</sup> In this procedure, the antimicrobial agents within the sample extract diffuse into the medium and interact with a plate that has been freshly inoculated with test organisms. Consequently, the resulting zones of inhibition exhibit a uniformly circular pattern due to the confluent growth, and the measurement of inhibition zone diameters is conducted in millimetres.

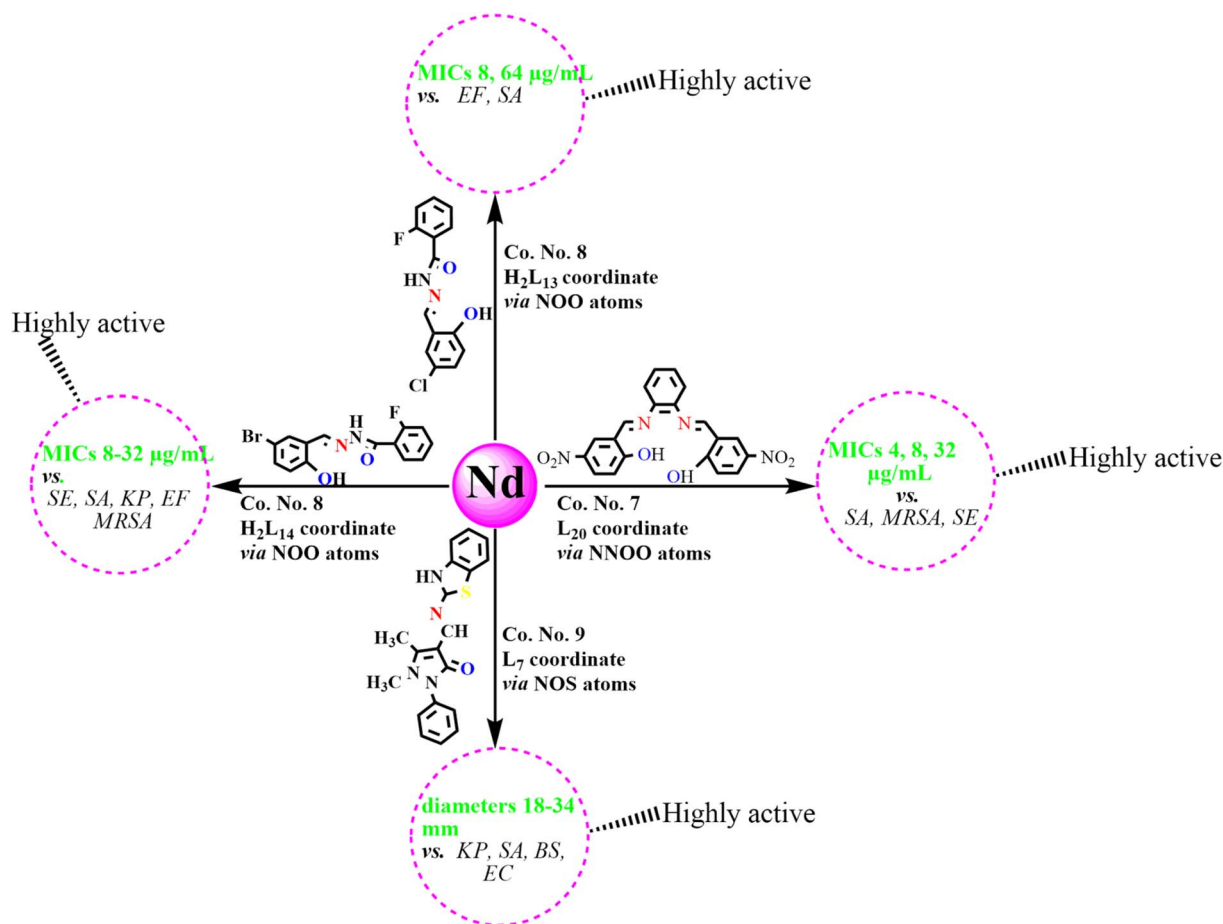
**6.1.3 Antimicrobial gradient method (E-test).** The E-test also known as 'Exponential gradient' method is a quantitative technique that has been developed for the purpose of evaluating

the antimicrobial resistance of G(+) and G(-) bacteria.<sup>154</sup> This method is based on creation of a concentration gradient of the antimicrobial agent tested in the agar medium. The E-test involves the use of a slim, inert and non-porous plastic strip. On one side of the strip (A), a scale present, indicating minimum inhibitory concentration (MIC) readings in  $\mu\text{g mL}^{-1}$ , accompanied by a two or three-letter code on the handle specifying the identity of the antibiotic. In this procedure, a previously inoculated agar surface with the test microorganism is overlaid with a strip containing an escalating concentration gradient of the antimicrobial agent, ranging from one end to the other.<sup>155</sup> This method is successfully employed for the determination of MIC value of antibiotics, antifungals and antimycobacterials.<sup>156</sup> This approach is focused on developing an antibacterial agent concentration gradient that is evaluated in an agar medium.

## 6.2 Dilution methods

This approach is widely used for determining Minimum Inhibitory Concentration (MIC) values, offering flexibility to calculate the concentration of the tested antimicrobial agent in either the agar (agar dilution) or broth medium (macro dilution or micro dilution). The quantitative measurement of antimicrobial activity against bacterial and fungal strains is achieved through either the broth or agar dilution method.<sup>157</sup>





Scheme 3 Most potent Nd(III)-Schiff base complexes against different bacterial strains.

**6.2.1 Agar dilution method.** The agar dilution methods do not involve the sophisticated equipment and are comparatively quick<sup>158</sup> involving basic microbiological facility. In this method, the test sample is incorporated at known concentrations into the agar, and once the agar has set, the bacteria are applied to its surface. The application of multiple bacterial species can be applied to individual dishes arranged with varying concentrations of the test sample, achieved by dividing the agar surface into wedges or squares. This configuration facilitates the screening of a substantial number of bacteria within a single assay run. Following a 24-hour incubation period, the presence or absence of bacterial growth on the extract/agar mixture is determined, and the results are expressed as a proportion relative to the control. It has been demonstrated that this technique is applicable for both antibacterial and antifungal susceptibility testing.<sup>152</sup>

**6.2.2 Broth dilution method.** Due to challenges associated with the partitioning of hydrophobic compounds in agar, a more precise method was developed and known as the broth dilution method.<sup>159</sup> In this method, bacterial cultures of specific bacteria are grown in test tubes containing test compounds in a liquid medium.<sup>160</sup> At regular time intervals (every 10 minutes or every hour) a sample is extracted, and the bacterial count (CFU) is calculated by serial dilution. The broth dilution

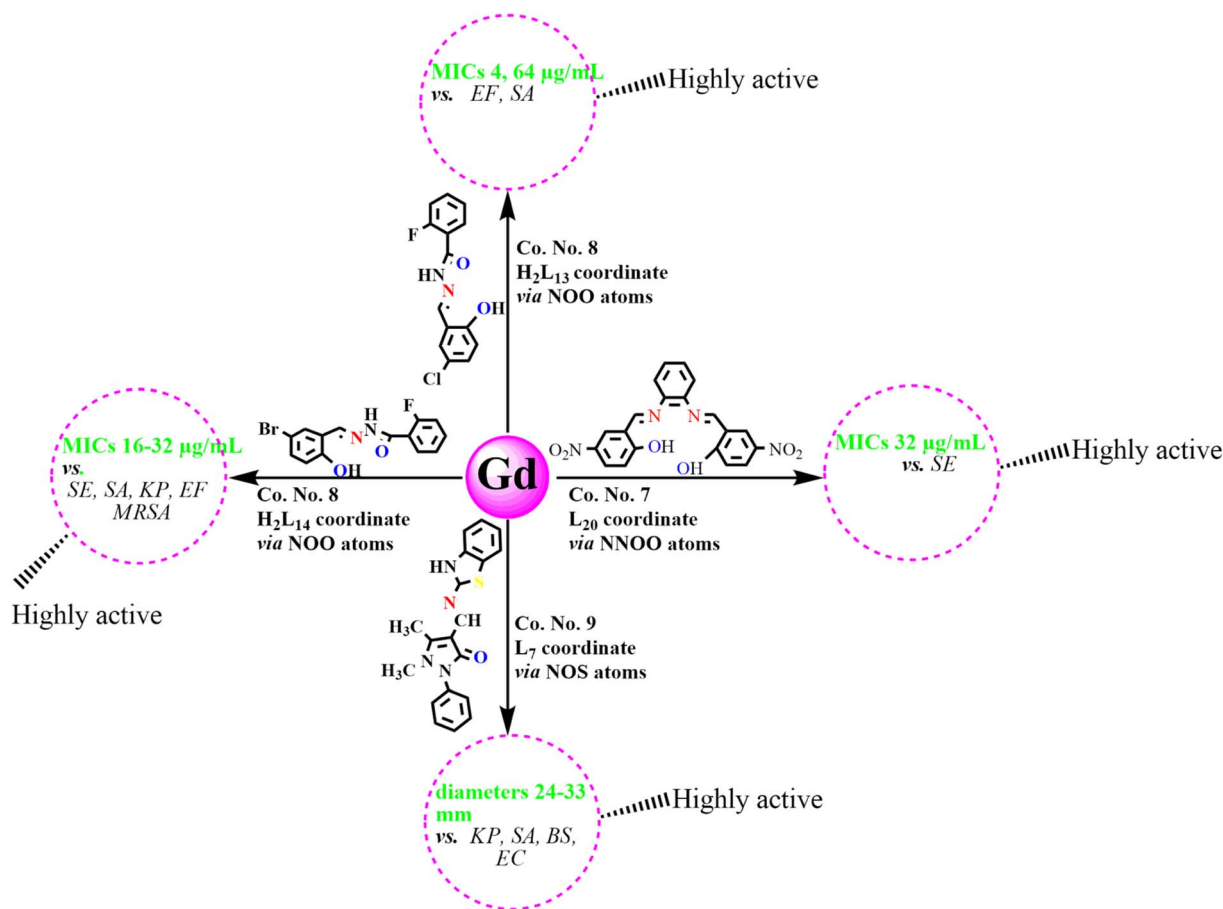
method has been shown to provide a considerably more comprehensive analysis of the antibacterial events over time in comparison to the single data point (24 h incubation) used in disc diffusion and agar dilution experiment. Apart from this, this approach has been demonstrated to offer several advantages, including the ability to determine the proportion of organisms destroyed at a specific period, as well as the ability to facilitate recovery from the effects of the test chemicals. However, the procedure may prove to be impractical when employed for the screening of numerous test chemicals, due to significant expenses in terms of time and resource expensive.<sup>161</sup> As with other testing methods, the incorporation of hydrophobic compounds and essential oils into the aqueous medium poses challenges. In the absence of a solid phase to trap these compounds, their rapid dispersion within the media is inevitable, resulting in the formation of layer across the surface.

## 7. Challenges and future directions

### 7.1 Current challenges

Despite considerable advances in the synthesis and evaluation of Schiff base-lanthanide complexes during 2018–2025, their transition from laboratory curiosity to practical antibacterial agents remains constrained by multiple challenges. While *in*





Scheme 4 Most potent Gd(III)-Schiff base complexes against different bacterial strains.

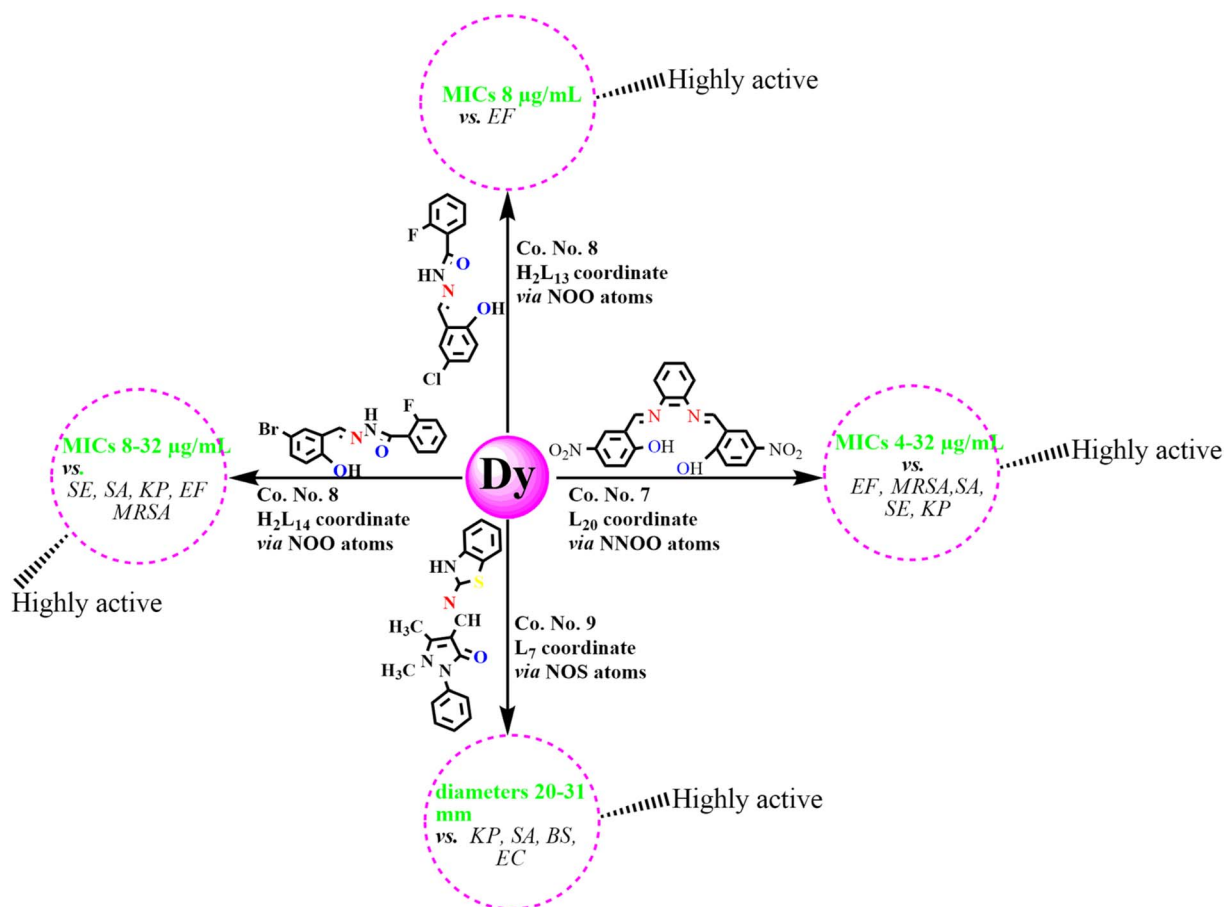
*vitro* results are promising, significant hurdles regarding solubility, toxicity, stability and translational applicability continue to limit their scope. A consistent limitation across reported studies is poor solubility and bioavailability. Most the Schiff bases, particularly L<sub>7</sub>, H<sub>2</sub>L<sub>13</sub>, and H<sub>2</sub>L<sub>14</sub>, feature extended aromatic scaffolds that confer lipophilicity but reduce solubility in aqueous solvent, limiting their biological applicability.<sup>72,90</sup> Even though these ligands and their complexes demonstrated strong activity against SA and KP, their hydrophobicity complicates formulation for *in vivo* delivery. The toxicity and selectivity shown by these complexes are still unresolved. Taha *et al.* (2024) reported that H<sub>2</sub>L<sub>6</sub> and its Ln(III) complexes exhibited moderate activity against EC and KP, but no effect against G(+) strains, suggesting that broad-spectrum selectivity is still lacking.<sup>70</sup> Stability under physiological conditions also poses a problem. Schiff base ligands are prone to hydrolysis and lanthanide complexes often undergo ligand exchange reactions. For instance, in the work of Mishra *et al.* (2022), Ln(III) complexes of L<sub>15</sub>-L<sub>16</sub> showed antibacterial effects against skin pathogens, yet their long term stability in biological systems was not reported.<sup>92</sup> Perhaps the most critical limitation is the absence of translational data. Most studies rely solely on agar diffusion or MIC assays. No reports have advanced into *in vivo* infection models, pharmacokinetics or preclinical trials. This gap

between bench chemistry and biomedical validation remains the largest bottleneck for clinical adoption.

## 7.2 Future perspectives

Research into Schiff bases and their lanthanide (Ln(III)) complexes has increasingly shown their promising antibacterial properties. However, despite these advancements, the transition from laboratory research to clinically applicable treatments remains limited. This highlights the need for a forward looking approach that addresses both the challenges and opportunities in this area. The future of antibacterial research involving Schiff base-lanthanide complexes will likely be driven by progress in sustainable synthesis methods,<sup>109</sup> targeted structural design, mechanistic understanding and pharmacological validation.<sup>162,163</sup> While Schiff bases and its Ln(III) complexes consistently showed activity mainly against G(+) bacteria, G(-) bacteria tend to be more resistant. The future work should be the selective targeting of G(-) bacteria by structural modifications of Schiff bases, such as adding amphiphilic groups or cationic moieties, to improve bacterial membrane penetration.<sup>109,163</sup> The existing literature suggest that lanthanide-Schiff base complexes may exert antibacterial effects through multiple mechanisms, including DNA binding, membrane disruption and enzyme inhibition.<sup>85,96</sup> The rational design of these

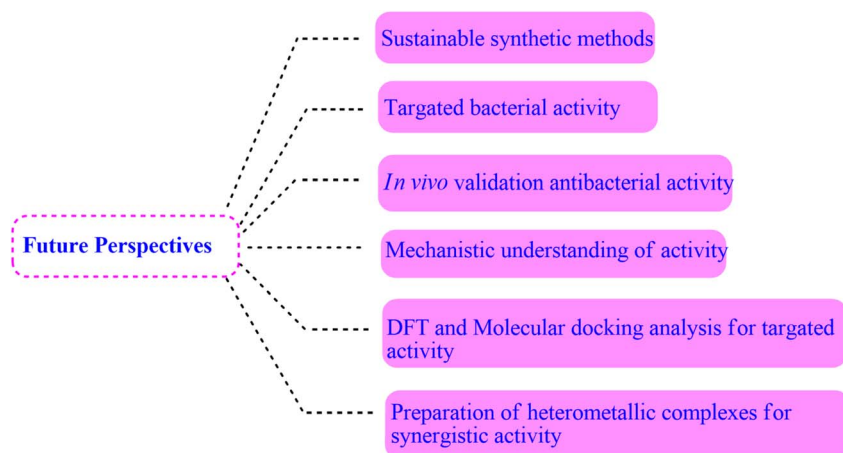




Scheme 5 Most potent Dy(III)-Schiff base complexes against different bacterial strains.

complexes with mechanistic guidance is very important for future works. The integration of biochemical assays, molecular docking and omics-based profiling can provide deeper insights into precise molecular targets of these complexes. The structural studies like X-ray crystallographic of ligand-protein interaction could further elucidate how specific coordination

environment drive antibacterial activity.<sup>164</sup> The pharmacokinetic and toxicological profiles of Schiff base and its lanthanide complexes remain insufficiently studied. For clinical translation, future research must assess solubility, stability, protein binding and bio-distribution.<sup>162,163</sup> *In vivo* validation is also essential as many studies are limited to *in vitro* assays such as



Scheme 6 Future scope of Schiff base and its Ln(III) complexes.



diameters of zone of inhibition, MIC and MBC tests, which do not fully capture biological complexity.<sup>37,165</sup> Another promising direction is the development of mixed-metal and hetero-bimetallic complexes. The combination of lanthanides with transition metals or other bioactive ions may provide synergistic effects by combining redox activity with unique coordination chemistry.<sup>166</sup> The pronounced ROS activity exhibited by Eu(III) and Dy(III) complexes indicates that the integration of redox-active centres with lanthanides could further promote ROS generation and thereby enhance antibacterial efficacy.<sup>167,168</sup> The computational approaches including density functional theory (DFT) and molecular docking can greatly accelerate drug discovery. However, these methods are rarely applied to correlate observed MIC values with mechanistic insights. For instance, Hussein *et al.* (2024) proposed that Ln(III) complexes with the L<sub>7</sub> Schiff base disrupt bacterial membranes, but this was inferred rather than confirmed through computational studies.<sup>72</sup> *In silico* predictions of stability, permeability and enzyme inhibition could shift research from trial-and-error synthesis toward rational design.<sup>169</sup> Additionally, scaling green and sustainable synthesis methods is important. Microwave-assisted and solvent-minimized approaches have been shown to produce Schiff bases rapidly with improved yields and lower environmental impact.<sup>170</sup> Adoption of microwave irradiation, solvent-free grinding, ultrasonic methods, or biomass-derived starting materials could improve sustainability in ligand preparation and complexation.

In conclusion, future research on Schiff bases and their lanthanide complexes is expected to focus primarily on the key aspects illustrated in Scheme 6.

## 8. Conclusion

Over the last seven years (2018–2025), the design and investigation of Schiff base ligands and their Ln(III) complexes as antibacterial drugs have progressed considerably. A consistent pattern appeared across this study, while free Schiff bases generally display only moderate antibacterial activity; their coordination with Ln(III) ions enhances lipophilicity, improves membrane penetration, and introduces additional mechanisms such as enzyme inhibition and reactive oxygen species (ROS) generation. As a result, many Ln(III)–Schiff base complexes exhibit greater antibacterial activity than the corresponding free ligands, although their activity still frequently lower than conventional standard antibiotics. The parent Schiff base's activity is increased after complexation with Ln(III) ions because of increased lipophilicity, which enables lanthanide(III) complexes to pass through the cell's lipid membranes and disrupt its normal function, ultimately resulting in cell death. Comparative studies reveals that Schiff bases like L<sub>7</sub>, H<sub>2</sub>L<sub>14</sub>, L<sub>20</sub>, HL<sub>30</sub>, HL<sub>32</sub> with Ln(III) ions particularly La(III), Nd(III), Gd(III), Tb(III) and Dy(III) are more consistently associated with strong antibacterial activity. The most active Ln(III) complexes tend to feature coordination number range 7–9 with donor sets involving N, O and S atoms that create stable and biologically reach architectures. Schiff bases bearing electron donating substituents, extended aromatic system and hydrophilic groups

have further shown to influence activity profiles. Despite these promising advances, the practical translation of Schiff base–lanthanide complexes remains constrained by key limitations, including poor aqueous solubility, limited stability under physiological conditions and the absence of comprehensive translational data beyond *in vitro* assay. Furthermore, activity against Gram-negative bacteria remains a bottleneck, likely due to permeability barriers in the outer membrane. Future developments in the subject would include the creation of mixed-metal or multinuclear systems, the use of green synthetic techniques to improve scalability and biocompatibility, and logical ligand design informed by computational modelling. Above all, converting these complexes into effective antibacterial medicines will require combining *in vitro* tests with mechanistic research and *in vivo* validation. Schiff base–lanthanide complexes, in summary, are a dynamic and adaptable class of substances having definite antibacterial potential. They provide new approaches to treating multidrug-resistant infections, even though they are not yet ready to take the place of traditional antibiotics. This is especially true if future studies continue to increase their selectivity, refine their structures, and close the crucial gap between bench and bedside.

## Author contributions

S. P.: investigation, conceptualization, writing original draft, methodology, formal analysis, data collection, review & editing. N. J.: validations, methodology, review & editing. A. N.: visualization, methodology, and reviewing. Urvashi: formal analysis, review & editing. M. K.: visualization, methodology, and reviewing. D. M.: formal analysis, visualization, review and editing. N. Y.: supervision, review & editing modification.

## Conflicts of interest

The authors declare no competing interests.

## Abbreviations

G(+)	Gram positive
G(–)	Gram negative
SA	<i>Staphylococcus aureus</i>
EF	<i>Enterococcus faecalis</i>
EC	<i>Escherichia coli</i>
PA	<i>Pseudomonas aeruginosa</i>
KP	<i>Klebsiella pneumonia</i>
BS	<i>Bacillus subtilis</i>
SAI	<i>Staphylococcus albus</i>
ML	<i>Micrococcus luteus</i>
MRSA	Methicillin resistant <i>staphylococcus aureus</i>
PV	<i>Proteus vulgaris</i>
ST	<i>Salmonella typhi</i>
SE	<i>Salmonella enteritidis</i>
PBA	<i>Propionibacterium acnes</i>
BC	<i>Bacillus cereus</i>
SF	<i>Shigella flexneri</i>
NG	<i>Neisseria gonorrhoeae</i>



AB	<i>Acinetobacter baumannii</i>
PM	<i>Proteus mirabilis</i>
SPy	<i>Streptococcus pyogenes</i>
BM	<i>Bacillus megaterium</i>
SAg	<i>Streptococcus agalactiae</i>
SM	<i>Serratia Marcescens</i>
SD	<i>Shigella dysenteriae</i>
KPA	<i>Klebsiella pseudomonas aeruginosa</i>
SF	<i>Streptococcus faecalis</i>
LM	<i>Listeria monocytogenes</i>
SP	<i>Streptococcus pneumonia</i>
PC	<i>Pseudomonas cepacicola</i>
PSy	<i>Pseudomonas syringae</i>
Ln	Lanthanide
DMF	Dimethylformamide
DMSO	Dimethyl sulfoxide
dbm	dibenzoylmethane
SAR	Structure–activity relationships

## Data availability

The data presented in this review are derived from previously published studies and have been extracted and summarized for inclusion in this manuscript. Relevant information is organized within the tables and figures and no new data were generated or analysed as part of this review. The original datasets can be accessed through the cited sources in the reference list, and readers are encouraged to consult those original publications for further details.

Supplementary information (SI): Table S1, summarizing reported Schiff bases and their Ln(III) complexes, the bacterial strains used for antibacterial evaluation, and relevant references. See DOI: <https://doi.org/10.1039/d5ra08181e>.

## References

- (a) World Health Organization, Antimicrobial Resistance, 2021, available at: <https://www.who.int/news-room/factsheets/detail/antimicrobial-resistance>, accessed March 21, 2023; (b) K. W. K. Tang, B. C. Millar and J. E. Moore, *Br. J. Biomed. Sci.*, 2023, **80**, 11387; (c) C. Llor and L. Bjerrum, *Ther. Adv. Drug Saf.*, 2014, **5**, 229–241; (d) I. H. Ifijen, P. Agyemang, E. Faderin, L. O. Odo, E. I. Okeke, D. I. Onugha, S. E. Obuba, O. Oluwafunke and C. Ogochukwu, *Next Mater.*, 2025, **8**, 100719; (e) K. L. Y. Christensen, R. C. Holman, C. A. Steiner, J. J. Sejvar, B. J. Stoll and L. B. Schonberger, *Clin. Infect. Dis.*, 2009, **49**, 1025.
- I. Cota, V. Marturano and B. Tylkowski, *Coord. Chem. Rev.*, 2019, **396**, 49.
- T. Dikid, S. K. Jain, A. Sharma, A. Kumar and J. P. Narain, *Indian J. Med. Res.*, 2013, **138**, 19.
- R. K. Obi, N. M. Orji, F. C. Nwanebu, C. C. Okangba and U. U. Ndubuisi, *Asian J. Exp. Biol. Sci.*, 2010, **1**, 271.
- S. Mohammed, *J. Vet. Med. Anim. Sci.*, 2023, **6**, 1132.
- L. H. Taylor, S. M. Latham and M. E. Woolhouse, *Philos. Trans. R. Soc. London, Ser. B*, 2001, **356**, 983.
- National Institute of Allergy and Infectious Diseases, Emerging and Re-emerging Infectious Diseases, 2008, available at: <http://www.naid.nih.gov/factsheet/infectiousdiseases.htm>.
- M. E. Woolhouse and S. G. Sequeria, *Emerging Infect. Dis.*, 2005, **11**, 1842.
- B. A. Brown-Elliott, K. A. Nash and R. J. Wallace Jr, *Clin. Microbiol. Rev.*, 2012, **25**, 545.
- T. M. Uddin, A. J. Chakraborty, A. Khusro, B. R. M. Zidan, S. Mitra, T. B. Emran, K. Dhama, M. K. H. Ripon, M. Gajdacs, M. U. K. Sahibzada and M. J. Hossain, *J. Infect. Public Health*, 2021, **14**, 1750.
- K. E. Jones, N. G. Patel, M. A. Levy, A. Storeygard, D. Balk, J. L. Gittleman and P. Daszak, *Nature*, 2008, **451**, 990.
- S. K. Fathalla, H. A. El-Ghamry and M. Gaber, *Inorg. Chem. Commun.*, 2021, **129**, 108616.
- H. R. van Doorn, *Medicine*, 2017, **45**, 798.
- S. Ahmed, M. Z. Ahmed, S. Rafique, S. E. Almasoudi, M. Shah, N. A. Che Jalil and S. C. Ojha, *BioMed Res. Int.*, 2023, **2023**, 5250040.
- N. Mishra, R. Yadav, K. Kumar, H. Pandey and R. Pandey, *J. Phys.: Conf. Ser.*, 2020, **1504**, 012002.
- A. F. Wady, M. B. Hussein and M. M. Mohammed, *Sch. Int. J. Chem. Mater. Sci.*, 2021, **4**, 46.
- I. B. Amali, M. P. Kesavan, V. Vijayakumar, N. I. Gandhi, J. Rajesh and G. Rajagopal, *J. Mol. Struct.*, 2019, **1183**, 342.
- E. Ritter, P. Przybylski, B. Brzezinski and F. Bartl, *Curr. Org. Chem.*, 2009, **13**, 241.
- N. H. Yarkandi, H. A. El-Ghamry and M. Gaber, *Mater. Sci. Eng., C*, 2017, **75**, 1059.
- R. El-Sharkawy and H. A. El-Ghamry, *J. Mol. Liq.*, 2019, **282**, 515.
- N. Channa, R. H. Khan, A. M. Moina, A. Bano, I. Saghir, C. Umedan, L. R. Nasira and Q. Samra, *J. Chem. Lett.*, 2024, **4**, 232.
- C. Alexander, Z. Guo, P. B. Glover, S. Faulkner and Z. Pikramenou, *Chem. Rev.*, 2025, **125**, 2269–2370.
- A. L. Gassner, C. Duhot, J.-C. G. Bünzli and A. S. Chauvin, *Inorg. Chem.*, 2008, **47**, 7802.
- S. V. Eliseeva and J.-C. G. Bünzli, *Chem. Soc. Rev.*, 2010, **39**, 189.
- P. Hermann, J. Kotek, V. Kubicek and I. Lukes, *Dalton Trans.*, 2008, **23**, 3027.
- E. Kusriani, F. Hashim, M. I. Saleh, R. Adnan, A. Usman, I. N. Zakaria, W. W. Prihandini, N. Putra and E. A. Prasetyanto, *J. Mater. Sci.*, 2020, **55**, 9795.
- R. Kumar, K. Seema, D. K. Singh, P. Jain, N. Manav, B. Gautam and S. N. Kumar, *J. Coord. Chem.*, 2023, **76**, 1065.
- S. P. Fricker and S. Fricker, *Chem. Soc. Rev.*, 2006, **35**, 524.
- K. L. Peterson, J. V. Dang, E. A. Weitz, C. Lewandowski and V. C. Pierre, *Inorg. Chem.*, 2014, **53**, 6013.
- L. Lekha, K. K. Raja, G. Rajagopal and D. Easwaramoorthy, *J. Organomet. Chem.*, 2014, **753**, 72.
- L. Zhu, B. Zhu, J. Luo and B. Liu, *ACS Mater. Lett.*, 2021, **3**, 77.



- 32 T. Zhang, X. Zhu, W. K. Wong, H. L. Tam and W. Y. Wong, *Chem.–Eur. J.*, 2013, **19**, 739.
- 33 M. T. Kaczmarek, M. Zabiszak, M. Nowak and R. Jastrzab, *Coord. Chem. Rev.*, 2018, **370**, 42.
- 34 C. S. Cutler, C. J. Smith, G. J. Ehrhardt, T. T. Tyler, S. S. Jurisson and E. Deutsch, *Cancer Biother. Radiopharm.*, 2000, **15**, 531.
- 35 A. H. Pathan, G. N. Naik, R. P. Bakale, S. S. Machakanur and K. B. Gudasi, *Appl. Organomet. Chem.*, 2012, **26**, 148.
- 36 V. Amani and F. Norouzi, *Chem. Pap.*, 2024, **78**, 1699.
- 37 J. Ceramella, D. Iacopetta, A. Catalano, F. Cirillo, R. Lappano and M. S. Sinicropi, *Antibiotics*, 2022, **11**, 191.
- 38 H. Schiff, *Ann. Chem. Pharm.*, 1864, **131**, 118–119.
- 39 P. A. Vigato and S. Tamburini, *Coord. Chem. Rev.*, 2004, **248**, 1717–2128.
- 40 (a) S. Cotton, in *Lanthanide and Actinide Chemistry*, John Wiley & Sons, Hoboken, NJ, 2006, pp. 35–60; (b) K. Binnemans, *Chem. Rev.*, 2009, **109**, 4283–4374; (c) R. E. Cramer, J. M. Rimsza and T. J. Boyle, *Inorg. Chem.*, 2022, **61**, 6120–6127; (d) S. Li, S. Jansone-Popova and D.-E. Jiang, *Sci. Rep.*, 2024, **14**, 11301.
- 41 Z. H. Chohan, *Appl. Organomet. Chem.*, 2006, **20**, 112–116.
- 42 J. E. Muraleedharan and K. P. Viswanathan, *Orient. J. Chem.*, 2025, **41**(1), 254.
- 43 S. Nagar, S. Raizada and N. Tripathi, *Results Chem.*, 2023, **6**, 101153.
- 44 M. T. Baig, M. T. Sayed, R. Aledamat, S. Hassan, A. AlReyashi, N. Sidiq and M. F. Mady, *BMC Chem.*, 2025, **19**, 201.
- 45 M. Draye, G. Chatel and R. Duwald, *Pharmaceuticals*, 2020, **13**, 23.
- 46 A. M. Hassan, A. O. Said, B. H. Heikal, A. Younis, W. M. Aboulthana and M. F. Mady, *ACS Omega*, 2022, **7**, 32418–32431.
- 47 A. Abd-El-Aziz, Z. Li, X. Zhang, S. Elnagdy, M. S. Mansour, A. ElSherif and A. S. Abd-El-Aziz, *Top. Curr. Chem.*, 2025, **383**, 8.
- 48 E. R. Trivedi, S. V. Eliseeva, J. Jankolovits, M. M. Olmstead, S. Petoud and V. L. Pecoraro, *J. Am. Chem. Soc.*, 2014, **136**, 1526.
- 49 T. Zhang, X. Zhu, C. C. Cheng, W. M. Kwok, H. L. Tam, J. Hao and K. L. Wong, *J. Am. Chem. Soc.*, 2011, **133**, 20120.
- 50 M. A. Katkova and M. N. Bochkarev, *Dalton Trans.*, 2010, **39**, 6599.
- 51 J. Jin, S. Niu, Q. Han and Y. Chi, *New J. Chem.*, 2010, **34**, 1176.
- 52 N. P. Ebosie, *J. Chem. Soc. Niger.*, 2025, **50**, 373–388.
- 53 H. E. Saad, G. M. Abu El Reash, M. Gaber, M. A. Hashem, Y. G. A. El-Reash, N. Y. Elamin and Y. S. El-Sayed, *BMC Genomics*, 2024, **25**, 162.
- 54 S. M. Abdel-Fatah, M. T. Basha, A. I. Al-Sulami, M. R. Shehata and L. H. Abdel-Rahman, *Appl. Organomet. Chem.*, 2025, **39**, e70192.
- 55 K. Zhang, D. Wang, S. Wu, C. Wang, Z. Yu and L. Zhang, *Struct. Chem.*, 2025, **36**, 213–221.
- 56 M. A. Subhan, M. S. Rahman, K. Alam and M. M. Hasan, *Spectrochim. Acta, Part A*, 2014, **118**, 944.
- 57 H. G. Sogukomerogullari, E. Basaran, R. A. Kepekci, B. Turkmenoglu, A. O. Sarioglu and M. Kose, *Polyhedron*, 2025, **265**, 117275.
- 58 A. A. Abdel Aziz and S. H. Seda, *J. Fluoresc.*, 2015, **25**, 1711.
- 59 D. Sahin, R. A. Kepekci, B. Turkmenoglu and S. Akkoc, *J. Biomol. Struct. Dyn.*, 2025, **43**, 3375.
- 60 B. G. Tweedy, *Phytopathology*, 1964, **55**, 910.
- 61 F. Chioma, O. Okpareke, S. N. Okafor and C. I. Ezugwu, *J. Mol. Struct.*, 2023, **1291**, 136070.
- 62 N. Raman, S. J. Raja and A. Sakthivel, *J. Coord. Chem.*, 2009, **62**, 691.
- 63 A. A. Emara, *Spectrochim. Acta, Part A*, 2010, **77**, 117.
- 64 S. H. Mahdi and L. K. A. Karem, *Inorg. Chem. Commun.*, 2024, **165**, 112524.
- 65 R. S. Abo-Rehab, E. A. Kasim, N. Farhan, M. S. Tolba, M. R. Shehata and E. M. Abdalla, *Appl. Organomet. Chem.*, 2024, **38**, e7622.
- 66 C.-Q. Miao, Y.-N. Ling, X.-Q. Ma, Y.-X. Chen, X.-J. Zhu, S.-R. Zhang and M. Fang, *Inorg. Chim. Acta*, 2024, **559**, 121782.
- 67 T. Meng, T. Liu, Q.-P. Qin, Z.-L. Chen, H.-H. Zou, K. Wang and F.-P. Liang, *Dalton Trans.*, 2020, **49**, 4404.
- 68 Y.-L. Song, Y.-T. Li and Z.-Y. Wu, *J. Inorg. Biochem.*, 2008, **102**, 1691.
- 69 T. Ahamad, N. Nishat and S. Parveen, *J. Coord. Chem.*, 2008, **61**, 1963.
- 70 Z. A. Taha, A. K. Hijazi, H. Abul-Futouh, W. Al-Momani, B. M. Alziqili, P. Liebing and W. Weigand, *J. Mol. Struct.*, 2024, **1316**, 139054.
- 71 Clinical and Laboratory Standards Institute, *Performance Standards for Antimicrobial Susceptibility Testing*, Wayne, PA, 2011, p. 100.
- 72 K. A. Hussein, N. Shaalan, A. K. Lafta and J. M. Al Akeedi, *Indones. J. Chem.*, 2024, **24**, 358.
- 73 K. A. Hussein and N. Shaalan, *Chem. Methodol.*, 2021, **6**, 103.
- 74 M. Alqasaimah, A.-A. Abu-Yamin, S. Matar, K. Al Khalyfeh, T. Rüffer, H. Lang and D. Taher, *J. Mol. Struct.*, 2023, **1274**, 134458.
- 75 K. Andiappan, A. Sanmugam, E. Deivanayagam, K. Karuppasamy, H. S. Kim and D. Vikraman, *Inorg. Chem. Commun.*, 2023, **150**, 110510.
- 76 K. Andiappan, A. Sanmugam, E. Deivanayagam, K. Karuppasamy, H. S. Kim and D. Vikraman, *Int. J. Biol. Macromol.*, 2019, **124**, 403.
- 77 K. Andiappan, A. Sanmugam, E. Deivanayagam, K. Karuppasamy, H. S. Kim and D. Vikraman, *Sci. Rep.*, 2018, **8**, 3054.
- 78 C. Xue, X. Xin, Y. Chang, Y.-J. Gao, J.-Y. Huang, H.-X. Qi and W.-M. Wang, *J. Mol. Struct.*, 2023, **1291**, 136058.
- 79 Z.-H. Shen, D.-F. Xu, N.-N. Cheng, X. Zhou, X. Chen, Y. Xu and Q. He, *J. Coord. Chem.*, 2011, **64**, 2342.
- 80 L. J. K. Boerner and J. M. Zaleski, *Curr. Opin. Chem. Biol.*, 2005, **9**, 135.
- 81 D.-F. Xu, S.-Z. Ma, G.-Y. Du, Q. He and D. Sun, *J. Rare Earths*, 2008, **26**, 643.



- 82 X.-Y. Xin, N. Qiao, C.-S. Cao, F.-J. Chen, W.-Y. Li, Y.-N. Ling and W.-M. Wang, *Inorg. Chim. Acta*, 2022, **541**, 121092.
- 83 E. A. M. Khalil and G. G. Mohamed, *Inorg. Chem. Commun.*, 2023, **153**, 110825.
- 84 H. F. Abd El-Halim, M. M. Omar and G. G. Mohamed, *Spectrochim. Acta, Part A*, 2011, **78**, 36.
- 85 A.-A. Abu-Yamin, M. S. Abduh, S. A. Saghir and N. Al-Gabri, *Pharmaceuticals*, 2022, **15**, 454.
- 86 I. P. Ejidike and P. A. Ajibade, *Bioinorg. Chem. Appl.*, 2015, **2015**, 1.
- 87 M. F. Abo-Ashour, W. M. Eldehna, R. F. George, M. M. Abdel-Aziz, M. M. Elaasser, N. M. A. Gawad and S. M. Abou-Seri, *Eur. J. Med. Chem.*, 2018, **160**, 49.
- 88 P. L. Ho, K. H. Chow, W. U. Lo and V. C. Cheng, *Int. J. Antimicrob. Agents*, 2011, **37**, 270.
- 89 H. S. Ibrahim, W. M. Eldehna, H. A. Abdel-Aziz, M. M. Elaasser and M. M. Abdel-Aziz, *Eur. J. Med. Chem.*, 2014, **85**, 480.
- 90 Z. A. Taha, T. S. Ababneh, A. K. Hijazi, S. M. Al-Aqtash, W. A. Al-Momani and I. Mhaidat, *J. Saudi Chem. Soc.*, 2022, **26**, 101400.
- 91 M. T. Kaczmarek, M. Zabiszak, M. Nowak and R. Jastrzab, *Coord. Chem. Rev.*, 2018, **370**, 42.
- 92 N. Mishra, K. Kumar, H. Pandey, S. R. Anand, R. Yadav, S. P. Srivastava and R. Pandey, *J. Saudi Chem. Soc.*, 2020, **24**, 925.
- 93 P. Ganapathi and K. Ganesan, *J. Mol. Liq.*, 2017, **233**, 452.
- 94 N. E. El-Gamel and K. A. Ali, *J. Mol. Struct.*, 2017, **1147**, 167.
- 95 K. M. Docherty Jr and C. F. Kulpa, *Green Chem.*, 2005, **7**, 185.
- 96 R. G. Deghadi and G. G. Mohamed, *Comments Inorg. Chem.*, 2022, **42**, 368.
- 97 W. H. Mahmoud, R. G. Deghadi and G. G. Mohamed, *J. Organomet. Chem.*, 2020, **917**, 121113.
- 98 W. H. Mahmoud, R. G. Deghadi, M. M. El Dessouky and G. G. Mohamed, *Appl. Organomet. Chem.*, 2019, **33**, e4556.
- 99 A. Albert, *J. Pharm. Sci.*, 1979, **68**, 662.
- 100 K. A. Hussein and N. Shaalan, *Indones. J. Chem.*, 2022, **22**, 1365.
- 101 S. M. Obaid, A. J. Jarad and A. A. Al-Hamdani, *J. Phys.: Conf. Ser.*, 2020, **1660**, 012028.
- 102 T. D. Tavares, J. C. Antunes, J. Padrao, A. I. Ribeiro, A. Zille, M. T. P. Amorim and H. P. Felgueiras, *Antibiotics*, 2020, **9**, 314.
- 103 A. H. Delcour, *Biochim. Biophys. Acta*, 2009, **1794**, 808.
- 104 E. Khalil, W. Mahmoud and G. Mohamed, *Egypt. J. Chem.*, 2021, **64**, 3555.
- 105 L. Shi, R.-Q. Fang, J.-Y. Xue, Z.-P. Xiao, S.-H. Tan and H.-L. Zhu, *Aust. J. Chem.*, 2008, **61**, 28.
- 106 S. V. Kumar, W. K. Lo, H. J. Brooks, L. R. Hanton and J. D. Crowley, *Aust. J. Chem.*, 2015, **69**, 489.
- 107 Z. A. Taha, A. K. Hijazi, A. Y. Al-Smadi, W. M. Al-Momani and F. Wedian, *Russ. J. Gen. Chem.*, 2021, **91**, 2292.
- 108 A. K. Hijazi, Z. A. Taha, A. Ibdah, I. M. Idris and W. M. Al-Momani, *Chem. Pap.*, 2021, **75**, 4611.
- 109 W. M. Al-Momani, Z. A. Taha, A. M. Ajlouni, Q. M. Shagra and M. A. Zouby, *Asian Pac. J. Trop. Biomed.*, 2013, **3**, 367.
- 110 K. B. Hussein and J. Zanco, *Pure Appl. Sci.*, 2021, **33**, 73.
- 111 J. D. L. Mosquera, A. A. Muriel, Y. Upegui, S. M. Robledo, M. T. Ramirez-Apan, D. Morales-Morales and D. Polo-Cerón, *Antibiotics*, 2021, **10**, 728.
- 112 J. M. Andrews, *J. Antimicrob. Chemother.*, 2001, **48**, 5.
- 113 J. M. Andrews, *J. Antimicrob. Chemother.*, 2002, **49**, 1049.
- 114 M. Arzanlou, W. C. Chai and H. Venter, *Essays Biochem.*, 2017, **61**, 49.
- 115 N. F. Mahmoud, W. H. Mahmoud and G. G. Mohamed, *Appl. Organomet. Chem.*, 2020, **34**, e5801.
- 116 Z. A. Taha, A. K. Hijazi and W. M. Al-Momani, *J. Mol. Struct.*, 2020, **1220**, 128712.
- 117 S. Paswan, A. Anjum, N. Yadav, N. Jaiswal and R. K. Singh, *J. Coord. Chem.*, 2020, **73**, 686.
- 118 N. Yadav, A. K. Jaiswal, K. K. Dey, V. B. Yadav, G. Nath, A. K. Srivastava and R. R. Yadav, *Mater. Chem. Phys.*, 2018, **218**, 10.
- 119 S. Paswan, N. Jaiswal, V. K. Modanawal, M. K. Patel and R. K. Singh, *Inorg. Chim. Acta*, 2020, **513**, 119955.
- 120 C. Nastasa, D. C. Vodnar, I. Ionuț, A. Stana, D. Benedec, R. Tămaian, O. Oniga and B. Tipericiu, *Int. J. Mol. Sci.*, 2018, **19**, 222.
- 121 J. D. L. Mosquera, A. A. Muriel and D. P. Cerón, *Univ. Sci.*, 2018, **23**, 141.
- 122 A. M. Ajlouni, Z. A. Taha, A. K. Hijazi and W. M. Al-Momani, *Appl. Organomet. Chem.*, 2018, **32**, e4536.
- 123 Z. A. Taha, A. M. Ajlouni and W. M. Al-Momani, *J. Lumin.*, 2012, **132**, 2832.
- 124 (a) K. Mohanan, R. Aswathy, L. P. Nitha, N. E. Mathews and B. S. Kumari, *J. Rare Earths*, 2014, **32**, 379; (b) M. Maciucă, A. C. Munteanu and V. Uivarosi, *Molecules*, 2020, **25**, 1347; (c) G. R. Choppin and D. R. Peterman, *Coord. Chem. Rev.*, 1998, **174**, 283; (d) J. Barańska, K. K. Szejn, M. Zabiszak, A. Grzeskiewicz, M. Skrobanska, M. Nowak, R. Jastrzab and M. T. Kaczmarek, *Int. J. Mol. Sci.*, 2025, **26**, 10379; (e) J.-C. G. Bünzli, *Chem. Rev.*, 2010, **110**, 2729; (f) J.-C. G. Bünzli and C. Piguet, *Chem. Rev.*, 2002, **102**, 1897; (g) B. Shyni, T. S. Sikha, J. P. Remiya, Y. M. Thasneem and S. S. Beevy, *J. Coord. Chem.*, 2023, **76**, 878; (h) O. Sun, T. Gao, J. Sun, G. Li, H. Li, H. Xu, C. Wang and P. Yan, *CrystEngComm*, 2014, **16**, 10460.
- 125 L. Zhang, D. Pornpattananangkul, C.-M. Hu and C.-M. Huang, *Curr. Med. Chem.*, 2010, **17**, 585.
- 126 B. Khameneh, R. Diab, K. Ghazvini and B. S. Bazzaz, *Microb. Pathog.*, 2016, **95**, 32.
- 127 C. Walsh, *Nature*, 2000, **406**, 775.
- 128 M. S. Refat, W. F. El-Hawary and M. A. Mohamed, *J. Mol. Struct.*, 2012, **1013**, 45.
- 129 B. G. Tweedy, *Phytopathology*, 1964, **55**, 910.
- 130 Y. Anjaneyula and R. P. Rao, *Synth. React. Inorg. Met.-Org. Chem.*, 1986, **16**, 257.
- 131 N. Nishat, S. Hasnain, S. Dhyani and J. Asma, *Coord. Chem.*, 2010, **63**, 3859.
- 132 A. E. Şabık, M. Karabork, G. Ceyhan, M. Tümer and M. Dıgırak, *Int. J. Inorg. Chem.*, 2012, **2012**, 1.
- 133 N. Dharmaraj, P. Viswanathamurthi and K. Natarajan, *Transition Met. Chem.*, 2001, **26**, 105.



- 134 Z. H. Chohan, M. Arif, A. Choukhtar and C. T. Supuran, *Bioinorg. Chem. Appl.*, 2006, **2006**, 1.
- 135 K. Siddappa, S. B. Mane and D. Manikprabhu, *Spectrochim. Acta, Part A*, 2014, **130**, 634.
- 136 E. L. Gavey and M. Pilkington, *Coord. Chem. Rev.*, 2015, **296**, 125.
- 137 Z. Shen, D. Xu, N. Cheng, X. Zhou, X. Chen, Y. Xu and Q. He, *J. Coord. Chem.*, 2011, **64**, 2342.
- 138 A. Hameed, M. Al-Rashida, M. Uroos, S. A. Ali and K. M. Khan, *Expert Opin. Ther. Pat.*, 2017, **27**, 63.
- 139 M. S. More, P. G. Joshi, Y. K. Mishra and P. K. Khanna, *Mater. Today Chem.*, 2019, **14**, 100195.
- 140 X. Liu and J.-R. Hamon, *Coord. Chem. Rev.*, 2019, **389**, 94.
- 141 K. Prajapati, P. Prajapati, M. Brahmabhatt and J. Vora, *Res. J. Life Sci., Bioinf., Pharm. Chem. Sci.*, 2018, **4**, 803.
- 142 A. Soroceanu and A. Bargan, *Crystals*, 2022, **12**, 1436.
- 143 T. Rakshit, A. Haldar, S. Jana, S. Raha, R. Saha and D. Mandal, *Results Chem.*, 2023, **6**, 101224.
- 144 A. Nijs, R. Cartuyvels, A. Mewis, V. Peeters, J. L. Rummens and K. Magerman, *J. Clin. Microbiol.*, 2003, **41**, 3627.
- 145 B. A. Brown-Elliott, J. M. Brown, P. S. Conville and R. J. Wallace Jr, *Clin. Microbiol. Rev.*, 2006, **19**, 259.
- 146 K. Syal, R. Iriya, Y. Yang, H. Yu, S. Wang, S. E. Haydel and N. Tao, *ACS Nano*, 2016, **10**, 845.
- 147 K. Das, R. K. Tiwari and D. K. Shrivastava, *J. Med. Plants Res.*, 2010, **4**, 104.
- 148 A. Taglietti, Y. A. Diaz Fernandez, E. Amato, L. Cucca, G. Dacarro, P. Grisoli and M. Patrini, *Langmuir*, 2012, **28**, 8140.
- 149 L. Fguira, S. Fotso, R. B. Ameer-Mehdi, L. Mellouli and H. Laatsch, *Res. Microbiol.*, 2005, **156**, 341.
- 150 K. Konate, J. F. Mavoungou, A. N. Lepengue, R. R. Aworet-Samseny, A. Hilou, A. Souza and B. M'Batchi, *Ann. Clin. Microbiol. Antimicrob.*, 2012, **11**, 18.
- 151 V. G. De Billerbeck, *Phytother. Res.*, 2007, **5**, 249.
- 152 N. S. Ncube, A. J. Afolayan and A. I. Okoh, *Afr. J. Biotechnol.*, 2008, **7**, 1797.
- 153 C. Valgas, S. M. Souza, E. Smania and A. Smania Jr, *Braz. J. Microbiol.*, 2007, **38**, 369.
- 154 R. Ashraf and N. P. Shah, *Int. Food Res. J.*, 2011, **18**, 837.
- 155 Y. F. Qiao, L. Du, J. Zhou, Y. Hu, L. Li, B. Li and Q. Zhao, *J. Coord. Chem.*, 2014, **67**, 2615.
- 156 V. Kuete, T. K. Tabopda, B. Ngamei, F. Nana, T. E. Tshikalange and B. T. Ngadjui, *S. Afr. J. Bot.*, 2010, **76**, 125.
- 157 M. A. Pfaller, D. J. Sheehan and J. H. Rex, *Clin. Microbiol. Rev.*, 2004, **17**, 268.
- 158 P. Cos, A. J. Vlietinck, D. Vlietinck and L. Maes, *J. Ethnopharmacol.*, 2006, **106**, 290.
- 159 J. N. Eloff, P. Masoko and J. Picard, *S. Afr. J. Bot.*, 2007, **73**, 667.
- 160 D. Ma, S. Panda and J. D. Lin, *EMBO J.*, 2011, **30**, 4642.
- 161 T. G. McCloud, *Molecules*, 2010, **15**, 4526.
- 162 D. Iacopetta, J. Ceramella, A. Catalano, A. Mariconda, F. Giuzio, C. Saturnino and M. S. Sinicropi, *Inorganics*, 2023, **11**, 320.
- 163 I. Pospieszna-Markiewicz, M. A. Fik-Jaskółka, Z. Hnatejko, V. Patroniak and M. Kubicki, *Molecules*, 2022, **27**, 8390.
- 164 L. Riccardi, V. Genna and M. De Vivo, *Nat. Rev. Chem.*, 2018, **2**, 100.
- 165 A. Omar and P. Nadworny, *Adv. Drug Delivery Rev.*, 2017, **112**, 61.
- 166 I. Kostova, *Curr. Med. Chem.*, 2024, **31**, 358.
- 167 A. Øwre, M. Vinum, M. Kern, J. Van Slageren, J. Bendix and M. Perfetti, *Inorganics*, 2018, **6**, 72.
- 168 S. Alfei, G. C. Schito, A. M. Schito and G. Zuccari, *Int. J. Mol. Sci.*, 2024, **25**, 7182.
- 169 S. Wankhede, A. Badule, S. Chaure, A. Damahe, M. Damahe and O. Porwal, *J. Adv. Sci. Res.*, 2025, **16**, 1.
- 170 S. B. Manjare, R. K. Mahadik, K. S. Manval, P. P. More and S. S. Dalvi, *ACS Omega*, 2022, **8**, 473.

